Journal of Neuroimmunology 337 (2019) 577048

Contents lists available at ScienceDirect

Journal of Neuroimmunology

journal homepage: www.elsevier.com/locate/jneuroim

An antibiotic depleted microbiome drives severe *Campylobacter jejuni*-mediated Type 1/17 colitis, Type 2 autoimmunity and neurologic sequelae in a mouse model

Phillip T. Brooks[a,c,d,e], Julia A. Bell[a,b,d], Christopher E. Bejcek[a,b], Ankit Malik[a,b], Linda S. Mansfield[a,b,d,e,*]

[a] *Comparative Enteric Diseases Laboratory, Michigan State University, East Lansing, MI, USA*
[b] *Departments of Microbiology and Molecular Genetics and Large Animal Clinical Sciences, Michigan State University, East Lansing, MI, USA*
[c] *Comparative Medicine Integrative Biology Graduate Program, Michigan State University, East Lansing, MI, USA*
[d] *College of Veterinary Medicine, Michigan State University, East Lansing, MI, USA*
[e] *Institute for Integrative Toxicology, Michigan State University, East Lansing, MI, USA*

ARTICLE INFO

Keywords:
Campylobacter jejuni
Guillain-Barré syndrome
Commensal microbiota
Mouse models
Autoimmunity
Gastrointestinal inflammation
Humanized microbiota model
Antimicrobial resistance

ABSTRACT

The peripheral neuropathy Guillain-Barré Syndrome can follow *Campylobacter jejuni* infection when outer core lipooligosaccharides induce production of neurotoxic anti-ganglioside antibodies. We hypothesized that gut microbiota depletion with an antibiotic would increase *C. jejuni* colonization, severity of gastroenteritis, and GBS. Microbiota depletion increased *C. jejuni* colonization, invasion, and colitis with Type 1/17 T cells in gut lamina propria. It also stimulated Type 1/17 anti-*C. jejuni* and -antiganglioside-antibodies, Type 2 anti-*C. jejuni* and -antiganglioside antibodies, and neurologic phenotypes. Results indicate that both *C. jejuni* strain and gut microbiota affect development of inflammation and GBS and suggest that probiotics following *C. jejuni* infection may ameliorate inflammation and autoimmune disease.

1. Introduction

Our aim in these studies was to determine the role of the gut microbiota in inflammatory and autoimmune disease in a murine model following infection with three *Campylobacter jejuni* strains isolated from patients with the peripheral autoimmune neuropathy Guillain Barré Syndrome (GBS). *Campylobacter* spp. are a leading cause of bacterial diarrheal illness (Scallan et al., 2011; Young et al., 2007). *C. jejuni* is responsible for approximately 1.3 million infections in the USA annually (CDC, 2014), especially from undercooked poultry and unpasteurized milk. *C. jejuni* causes fever, vomiting and diarrhea in most patients, which are debilitating but self-limiting within 7–10 days (Young et al., 2007). Occasionally, autoimmune diseases arise following exposure to *C. jejuni*, including inflammatory bowel disease (Kim et al., 2009), Reiter's arthritis (Garg et al., 2008), and the peripheral neuropathies Guillain-Barré and Miller-Fisher syndromes (GBS; MF) (Hughes and Rees, 1997; Yuki, 2012). *C. jejuni* was recently designated a serious antimicrobial resistance threat by the Centers for Disease Control and Prevention (CDC) (Centers for Disease Control and Prevention, 2013). Antibiotic resistant (AR) *C. jejuni* have been suggested to cause more severe infections requiring lengthier hospitalizations when compared to antibiotic susceptible infections (Moore et al., 2006). In addition, it has been suggested that more severe enteric disease may be more likely to lead to subsequent GBS (Gruenewald et al., 1991; Schonberg-Norio et al., 2010; Zia et al., 2003).

We have shown that untreated C57BL/6 IL-10$^{-/-}$ mice infected with *C. jejuni* GBS patient strains are susceptible to mild T cell mediated colitis and develop anti-ganglioside antibodies confirming autoimmunity (Malik et al., 2014). It is well known that manipulation of the resident gut microbiota can significantly impact host-susceptibility to pathogen colonization and subsequent enteritis mediated by colonization resistance (Kamada et al., 2013). Disruption of the resident gut microbiota with antibiotics increased susceptibility to *C. jejuni* colonization and enteric disease in two mouse models (O'Loughlin et al., 2015a; Stahl et al., 2014). Thus, we hypothesized that depleting the gut microbiota of C57BL/6 IL-10$^{-/-}$ mice with the broad spectrum antibiotic cefoperazone and then infecting them with *C. jejuni* GBS-associated isolates innately resistant to cefoperazone would (1) increase *C. jejuni* colonization, (2) increase the severity of host gastrointestinal lesions, and (3) increase levels of antibodies cross-reactive with neuronal

* Corresponding author at: Michigan State University, 181 Food Safety and Toxicology Building, 1129 Farm Lane, East Lansing, MI 48824, USA.
E-mail address: mansfie4@cvm.msu.edu (L.S. Mansfield).

https://doi.org/10.1016/j.jneuroim.2019.577048
Received 1 May 2019; Received in revised form 1 September 2019; Accepted 2 September 2019

gangliosides compared to both infected and uninfected untreated controls.

2. Materials and methods

2.1. Campylobacter jejuni strains and inoculum preparation

C. jejuni strains 260.94 (ATCC BAA-1234) and HB93-13 (ATCC 700297) were obtained from the American Type Culture collection (Manassas, VA). *C. jejuni* D8942 was obtained from the Centers for Disease Control (Atlanta, GA). All three strains used in these experiments were isolated from patients with Guillain-Barré syndrome (Jackson et al., 2013; Prendergast et al., 1998; Sheikh et al., 1998b). Strain HB93-13 was originally isolated from feces of an 8-year-old boy in China diagnosed with the acute motor axonal neuropathy (AMAN) form of GBS, while strain 260.94 was isolated from a patient of the Red Cross Children's hospital of Cape Town, South Africa, diagnosed with the acute inflammatory demyelinating polyneuropathy (AIDP) form of GBS. Strains HB93-13 and 260.94 both possess GM1 ganglioside mimics, while HB93-13 also has a GD1a mimic (Louwen et al., 2013); D8942 ganglioside mimicry is unknown. Inocula were prepared as described previously and checked for purity by Gram stain and > 90% darting motility by dark field microscopy (Mansfield et al., 2007).

2.2. Mouse model

All procedures involving animals were performed in accordance with the recommendations described in the Guide for the Care and Use of Laboratory Animals of the National Institutes of Health under protocols approved by the Michigan State University Institutional Animal Use and Care Committee (approval numbers 06/12-107-00 and 06/15-101-00). B6.129P2-IL-10^{tm1Cgn}/J (referred to here as C57BL/6 IL-10$^{-/-}$) mice were obtained from Jackson Laboratories (Bar Harbor, ME), a breeding colony was established in a *Campylobacter/Helicobacter*-free facility, and offspring were used for all experiments described here. Mice were housed in specific-pathogen-free conditions, fed an irradiated mouse diet (mouse breeder diet 7904; Harlan Teklad, Indianapolis, IN), kept on autoclaved bedding, and given filter sterilized water (autoclaved water in bottles for weanlings) in a limited-access room. PCR assays specified by Jackson Laboratories were used to confirm mouse genotypes both before and after experiments (https://www2.jax.org/protocolsdb/f?p=116:2:27254394395538::NO:2:P2_MASTER_PROTOCOL_ID,P2_JRS_CODE:2631,002251).

Experimental mice were screened for colitogenic bacteria including *Campylobacter* spp. (Linton et al., 1996), *Helicobacter* spp. (Riley et al., 1996), *Enterococcus faecalis* (Dutka-Malen et al., 1995), and *Citrobacter rodentium* (McKeel et al., 2002) using DNA isolated from fecal samples both prior to and at the conclusion of the experiment. The screening assays used were 16S rRNA gene PCR assay for *Campylobacter* spp. and *Helicobacter* spp., *espB* gene-specific PCR for *C. rodentium*, and *ddl* gene-specific PCR for *E. faecalis*. Dedicated sentinel mice were used to assess extraneous infection with bacterial, protozoan and viral agents (Charles River Laboratories, Wilmington, MA) and were monitored by the MSU Campus Animal Resources (CAR). Once mice reached 7 weeks of age they were transferred to the University Research Containment Facility for the following experiments.

2.3. Experimental designs

Three experiments with similar designs were conducted: the Pilot experiment and experiment 1 were concluded 5 at weeks post infection (PI); experiment 2 was concluded at 7 weeks PI (Table 1). In all three experiments, ten to 12-week-old C57BL/6 IL-10$^{-/-}$ mice received either sterile drinking water or 0.5 mg/mL cefoperazone (CPZ) in sterile drinking water for the duration of the experiment. Seven days after initiating CPZ treatment, mice receiving CPZ or normal drinking water were inoculated by oral gavage with 0.2 mL of either tryptone soya broth (TSB) or approximately 1×10^{10} cfu *C. jejuni* suspended in TSB. Administration of CPZ in sterile drinking water or antibiotic-free drinking water continued until euthanasia. Trained animal handlers monitored food, water, and general animal welfare daily. In order to limit avoidable discomfort, distress, pain, and injury all animals were monitored for clinical signs of disease twice daily after clinical signs appeared based on a scoring sheet developed for this purpose (Mansfield et al., 2007; St Charles et al., 2017). Each clinical sign observed had a point designation. Upon each scoring all points were added and if the sum was 9 or above animals were humanely euthanized to prevent suffering. Thus, a standardized humane endpoint was established. At 5 weeks PI (Pilot and experiment 1), 7 weeks PI (experiment 2), or at the humane endpoint, mice were administered an overdose of CO_2 in a sealed chamber according to guidelines of the AVMA (Leary et al., 2013). After euthanasia we also ruptured the diaphragm or thoracic wall to ensure that the mice would not revive.

Table 1
Distribution of mice in pilot, experiment 1, and experiment 2.

GROUP	NO. OF MICE	WEEKS PI
Pilot		
TSB	5	5
260.94	5	
260.94 + CPZ	4	
Experiment 1		
TSB	4	5
CPZ	5	
260.94	4	
260.94 + CPZ	5	
D8942	5	
D8942 + CPZ	4	
Experiment 2		
TSB	8	7
CPZ	8	
HB93-13	8	
HB93-13 + CPZ	7	

Table represents the treatment groups and number of animals per treatment group for all experiments at the time of inoculation. n = number of animals.

2.4. Necropsy and sample collection

A fecal sample was collected prior to euthanasia. Mice were euthanized, weighed and quickly prepared for necropsy. Blood was obtained by cardiac puncture and immediately mixed with 0.68% sodium citrate. Any instance of gross pathological change in the GI tract was recorded. Thickened (TW) or enlarged (ENL) colon or cecum walls and

bloody intestinal contents were observed and recorded at necropsy. Gross pathological findings were graded as follows: Grade 0 = no gross pathology detected, Grade 1 = thickened wall (TW) or enlarged (ENL) colon or cecum, Grade 2 = TW or ENL colon and cecum, Grade 3 = TW or ENL colon and cecum and bloody feces or luminal contents. Plasma was collected after centrifugation and quickly stored at −80 °C until further analysis could be performed. The colon and cecum were divided into 3 sections; one section of each organ was stored in formalin, flash frozen, or streaked on tryptone soya agar plates supplemented with 20 μg CPZ per mL, 10 μg vancomycin per mL, and 2 μg amphotericin B per mL (TSA-CVA) (all antibiotics from Sigma-Aldrich, St. Louis, MO) and incubated in a sealed container with a Campy*Gen* sachet for 48 h at 37 °C.

2.5. Quantification of C. jejuni in the cecum and colon

Small snips of cecum and colon tissue were taken and streaked on TSA-CVA plates. Semi-quantitative analysis of *C. jejuni* growth on these plates were judged using a standardized scoring system: 0 (no growth), 1 (1–20 CFU), 2 (20–200 CFU), 3 (200–400) and 4 (confluent growth) (Mansfield et al., 2007).

2.6. Preparation of the ileocecocolic junction (ICCJ), histopathology scoring and C. jejuni specific immunohistochemistry

Tissue samples previously fixed in 10% neutral buffered formalin were processed and vacuum infiltrated with paraffin in the Sakura VIP 2000 tissue processor; followed by embedding with the ThermoFisher HistoCentre III embedding station. Once blocks were cooled, excess paraffin was removed from the edges; placed on a Reichert Jung 2030 rotary microtome, faced to expose the tissue sample, and sectioned at 4–5 μm. Sections were dried at 56 °C in a slide incubator for 2–24 h. Slides were removed from the incubator and stained with a routine Hematoxylin and Eosin (H & E) method as follows: two changes of xylene – 5 min each, two changes of 100% ethanol – 2 min each, two changes of 95% ethanol – 2 min each, running tap water rinse for 2 min, Hematoxylin (Cancer Diagnostics – Durham, NC) for 1 ½ minutes followed directly by a 10–15 s differentiation in 1% aqueous glacial acetic acid and running tap water for 2 min to enhance nuclear detail. Upon completion of the running tap water step, slides were placed in one change of 95% ethanol – 2 min, 1% Alcoholic Eosin-Phloxine B – 2 min to stain cytoplasm, one change of 95% ethanol for 2 min, four changes of 100% ethanol – 2 min each, four changes of xylene – 2 min each followed by coverslipping with synthetic mounting media for permanent retention and visualization with light microscopy. Scoring of the distal ileum, cecum and proximal colon was conducted as described in Mansfield et al., 2007. Briefly, the lumen, epithelium, lamina propria and submucosa of the ICCJ of each mouse were observed for histopathological changes by an investigator (LSM) blinded to sample identity and a score from 1 to 41 was assigned based on the lesions (Mansfield et al., 2007). Another section of the ICCJ was sectioned and prepared for *C. jejuni* specific immunohistochemistry using a rabbit polyclonal antibody against *C. jejuni* (US Biologicals, Swampscott, MA) diluted 1:500 with normal antibody diluent (Scytek, Logan, UT) according to a previously published protocol (Mansfield et al., 2007).

2.7. Assessment of anti-C. jejuni and anti-ganglioside antibodies by enzyme-linked immunosorbent assay (ELISA)

Antibodies reactive with GM1 (Sigma-Aldrich), GD1a (USBio, Salem, MA) and a crude *C. jejuni* protein preparation were measured via indirect ELISA. Biotinylated goat anti-mouse secondary antibodies (Southern Biotech Birmingham, AL) were used to determine IgG subclasses (IgG1, IgG2b or IgG2c)(Mansfield et al., 2007; St Charles et al., 2017).

2.8. Collection of nerves and dorsal root ganglia and immunohistochemistry

We collected the sciatic nerve and 1 to 3 dorsal root ganglia from experimental mice for histological and morphological analysis. These structures were exposed by dissection at necropsy, the mouse carcass was fixed in formalin for 24 h and switched to 60% ethanol thereafter, and the structures further dissected and embedded en bloc in paraffin in order to assess the segmental nature of any GBS lesions (St Charles et al., 2017). Slides were prepared by the Michigan State University Investigative Histopathology Laboratory. Four-micron sections were placed on charged slides and dried at 56 °C overnight. Slides were subsequently deparaffinized in xylene and hydrated through descending grades of ethyl alcohol to distilled water. One section was stained with routine Hematoxylin and Eosin for assessment of inflammatory infiltrate composition, distribution and severity; this section was also evaluated for percentage of myelin sheath loss. The scoring criteria are explained in detail previously (St Charles et al., 2017). For F4/80 staining, slides were placed in Tris Buffered Saline (TBS) pH 7.4 (Scytek Labs – Logan, UT) for 5 min for pH adjustment. Following TBS, Epitope Retrieval was performed using Citrate Plus Retrieval Solution pH 6.0 (Scytek) in a vegetable steamer for 30 min followed by a 10-min countertop incubation and several changes of distilled water. Following pretreatment, standard avidin-biotin complex staining steps were performed at room temperature on the DAKO Autostainer. All staining steps were followed by two-minute rinses in Tris Buffered Saline and Tween 20 (Scytek). After blocking for non-specific protein with Normal Rabbit Serum (Vector Labs – Burlingame, CA) for 30 min; sections were incubated with Avidin / Biotin blocking system for 15 min each (Avidin D – Vector Labs / d-Biotin – Sigma-Aldrich). Primary antibody slides were incubated for 60 min with the Monoclonal Rat anti-Mouse F4/80 antibody diluted at 1:100 (AbD Serotec – Raleigh, NC) in Normal Antibody Diluent (NAD) (Scytek). Then, slides were incubated with biotinylated Rabbit anti-Rat IgG (H + L) Mouse Absorbed antibody prepared at 10.0 μg/mL in NAD and incubated for 30 min; followed by incubation in R.T.U. Vector Elite Peroxidase Reagent (Vector) for 30 min. Reaction development utilized Vector Nova Red Kit peroxidase chromogen incubation for 15 min followed by counterstaining in Gill 2 Hematoxylin (Cancer Diagnostics – Durham, NC) for 30 s. Thereafter slides underwent differentiation, dehydration, clearing and mounting with Permount mounting media. F4/80 stained cells were counted and normalized for tissue area using ImageJ version 2.0.0-rc43/1.50e (Caroline et al., 2012).

2.9. Preparation of lamina propria leukocytes and characterization by flow cytometry

A 3 cm segment of proximal colon tissue was collected from each mouse and held in RPMI 1640 containing 10% fetal bovine serum (FBS) (Sigma-Aldrich) until processing (30 mins). Epithelial cells were isolated by washing and cutting the colon into 1 cm pieces and incubating the pieces in calcium- and magnesium-free Hanks Buffered Saline Solution (HBSS) supplemented with 5% FBS and 5 mM EDTA while shaking at 150 rpm and 25 °C for 30 min. Tissues were then incubated in RPMI 1640 containing 10% FBS, 0.5 mg/mL collagenase type IV (Sigma-Aldrich), and 0.5 mg/mL DNase I (Sigma-Aldrich) while shaking at 150 rpm and 37 °C for 1 h. Liberated cells were filtered through a 100 μm nylon cell strainer (Falcon). Isolated cells were separated by a 40/80% discontinuous Percoll (GE Healthcare Life

Sciences) gradient. Prior to immunostaining, cells were re-stimulated with phorbol 12-myrisate 13-acetate (Sigma Aldrich) and ionomycin (BD Biosciences). Cytokine secretion was inhibited with brefeldin A (BD Biosciences) and BD GolgiStop™ (monensin) (BD Biosciences). Thereafter, cells were stained with anti-mouse CD19 PerCP-Cyanine5.5 (eBioscience) for B-cells, anti-mouse CD3e PerCP-Cyanine5.5 (eBiosciences) for T-cells, anti-mouse CD4 FITC (eBiosciences) for T-helper cells, interferon gamma (PE/Cy7) (eBioscience), and interleukin-4 (PE) (BD Biosciences). All cells were gated on a $CD^{-}19$ $CD3^{+}$ gate. Cell viability was assessed via trypan blue staining and forward and side scatter. At least 90% cell viability was required for inclusion.

2.10. Assessing neurologic phenotype in mice

In all experiments, each mouse was evaluated daily for the features/clinical signs listed in a clinical score sheet (St Charles et al., 2017). These included eating/drinking, respiratory rate, rough hair coat, dehydration, hunched posture, diarrhea, movement, difficulty rearing, muscle mass loss in hind leg, and tremors among other signs. Once mice were assessed from a distance, mice showing signs were restrained and examined including capillary refill time or simple neurologic clinical assessments depending upon the presentation. Evaluating of each clinical sign results in a score for that feature. When finished all scores are added together. If the total comes to > 9, this triggers automatic euthanasia as a humane endpoint.

Examination of mice for neurologic phenotypes was conducted in Experiment 2 at time zero and then at weekly intervals after infection. Open field testing was used to provide qualitative and quantitative measures of general locomotor activity, ability to explore the environment, balance and coordination. Thus, motor and proprioceptive deficits were observable while sensory abilities were not assessed. Mice were placed in a clear plastic container divided into four quadrants and were videotaped for a period of 2 min. Mice were untouched and unstimulated by noise or visual cues during the observation period, and the container was disinfected after each mouse tested. Mice were assessed for the number of rears and quadrants crossed, stride length, wide gait stance, splaying of either hind limb (wide hind limb foot angle), rear foot drags and knuckling. While being assessed for movement, mice were also assessed for respiratory effort. If mice displayed altered respiration, the number of deep inspirations were counted to determine whether respiratory distress was occurring. Humane endpoints were assessed as described previously (St Charles et al., 2017).

Mice were assessed for tail suspension test and clasping/grip test as described previously (Hatzipetros et al., 2015). We conducted a tail suspension test to examine motor control over the hind limbs. Mice were held by the base of the tail and videotaped to determine if they orient normally to the ground and exhibit normal limb extension and control. Normal mice suspended gently by the tail look toward the ground and reach with all four limbs extended and held in a steady manner. If abnormal on the tail suspension test, 1) one or both of the mouse's hindlimb(s) present an abnormal splay, i.e., are collapsed or partially collapsed toward lateral midline, or 2) hindlimbs tremble during tail suspension, or 3) the hindlimb(s) are retracted/clasped (Hatzipetros et al., 2015). Spontaneous flexor and extensor spasms were also counted if present. Any one of these abnormal presentations would result in a score of one for this feature. Mice then had a pen placed between the hindlimbs and observed for ability to grip the object. This test was repeated 3–4 times to distinguish if an abnormal flex or splay was in fact a neurological weakness. Phenotype data was collected with knowledge of the infectious status of each mouse to prevent transmission between groups of mice. Once data was collected, it was blinded to mouse identity by one investigator (PTB) and scored for phenotype by a veterinarian that did not participate in the phenotyping (LSM). The final data were analyzed by JAB and the group identity, treatment status and phenotyping results of the mice revealed, so comparisons between groups could be made.

2.11. Statistical analyses

Pilot study data analyses were conducted using the Kruskal-Wallis non-parametric one-way analysis of variance and Dunn's post-test when appropriate. Experiment 1 and 2 data analyses were conducted using a Kruskal-Wallis test on ranks and Dunn's post-test when appropriate. Histopathology data from the ICCJ were analyzed with the Kruskal-Wallis test on ranks for all experiments. If statistical significance was achieved, pairwise comparisons were made with Fishers Exact Test (http://vassarstats.net/fisher2x3.html) and corrected for multiple comparisons by implementing Holmes step-down method (Ludbrook, 1998). Scores were grouped in a 2-way table assigned a grade 0 (≤ 9), 1 ($10-20$) or 2 (> 20). Unless otherwise noted statistical analyses were performed using GraphPad Prism 6.0 h for Mac OS X, GraphPad Software, La Jolla California USA. Standard deviations for anti-ganglioside antibody and F4/80 comparative analyses were calculated with the STDEV·P function in Microsoft Excel for Mac version 15.15. Plasma samples were considered positive for *Campylobacter,* GM1, or GD1a antibodies an OD_{450} value two or more standard deviations above the mean value for plasma from uninfected, untreated controls was obtained (Malik et al., 2014).

3. Theory/rationale

GBS is currently held to be the result of antibody attack on peripheral nerves; development of such antibodies can be triggered either spontaneously or by infection with any of several bacterial and viral pathogens (Yuki and Hartung, 2012). The most common preceding infection is *Campylobacter jejuni;* other triggering pathogens include *Hemophilus influenzae*, *Mycoplasma pneumoniae*, influenza virus, Epstein Barr virus, cytomegalovirus (van den Berg et al., 2014)(van den Berg et al) and Zika virus (Uncini et al., 2017). These pathogens carry surface molecules that mimic molecules found on the surfaces of peripheral neurons; “autoantibodies” triggered by infection are thought to bind to the mimicked neuronal molecules and the resulting antigen: antibody complexes are thought to trigger attack by phagocytes such as macrophage (Willison et al., 2016). Anti-ganglioside antibodies are elicited following infection by some *C. jejuni* strains in response to carbohydrate structures resembling gangliosides found on the outer core of the *C. jejuni* lipo-oligosaccharide (LOS); only those *C. jejuni* strains carrying LOS that mimics neuronal gangliosides are thought to trigger autoantibody formation (Sheikh et al., 1998a; Yuki et al., 1993). Variation in type and degree of anti-ganglioside antibody elicitation in response to *C. jejuni* infection has been shown by our lab previously (Malik et al., 2014). This response is affected by differences in ganglioside mimicry and is correlated with genetic variation in LOS loci (Gilbert et al., 2002; Houliston et al., 2011; Parker et al., 2005).

IgG1 antibodies are of particular interest because previous reports on GBS patients have identified GM1 IgG1 antibodies as predictors of severe outcomes and prolonged recovery in humans (Koga et al., 2003). Because *C. jejuni* HB93-13 elicited significant IgG1 anti-ganglioside antibody responses in previous work (Malik et al., 2014), we expected that these responses would be repeated here and would be exacerbated by antibiotic treatment, which is what was observed. Regardless, other IgGs (such as IgG3 have stronger C1q binding than IgG1 molecules, however IgG1 has been shown to induce more potent cell damage because it situates the C1q binding site more proximal to the cell surface

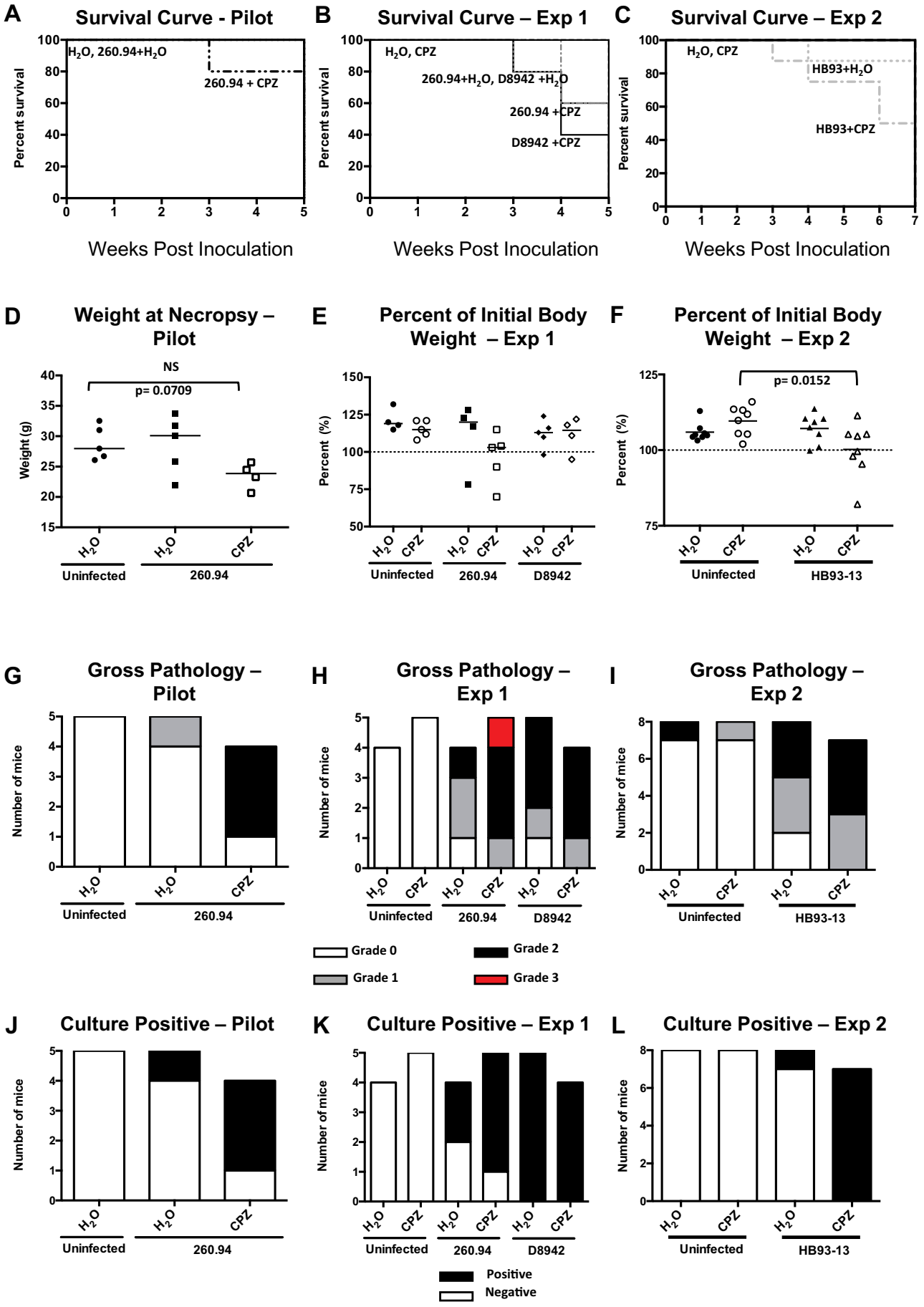

(caption on next page)

Fig. 1. Survival curve, endpoint body weight, gross pathology and culturable *C. jejuni.* C57BL/6 IL-10$^{-/-}$ mice were mice were inoculated with TSB or *C. jejuni* 260.94, D8942, or HB93-13 in three separate experiments and euthanized at 5-weeks (pilot and experiment 1), 7 weeks (experiment 2) or at the humane endpoint. Mice received sterile drinking water or 0.5 mg/mL CPZ in sterile drinking water for 7 days prior to infection; antibiotic treatment continued for the duration of the experiment. Panels A, B, and C) Survival curves, D) Body weight at necropsy, E and F) percent of initial body weight, G, H and I) gross pathological changes in the colon, cecum and lymph nodes (Grades 0 through 3 defined in Materials and Methods), J, K and L) number of culture positive mice at necropsy. Data represent 4–5 mice per group (pilot and experiment 1) or 7–8 mice per group (experiment 2) and were analyzed by the Kruskal-Wallis test on ranks and Dunn's Post test. In panel D, E, and F each symbol represents a single animal; bars represent group medians. NS, not significant.

(Melis et al., 2015). More work is needed to understand the exact mechanism of nerve damage in this model.

Manipulation of the gut microbiota has been critical to the development of several pathogen infection models, including *Clostridium difficile* (Antonopoulos et al., 2009; Theriot et al., 2014) and *Salmonella enterica* Typhimurium (Sekirov et al., 2008) murine models. In previous studies, limited flora mice (Chang and Miller, 2006), vancomycin treated mice (Stahl et al., 2014), and ampicillin treated mice (O'Loughlin et al., 2015a) were shown to be more susceptible to *C. jejuni* colonization and enteritis. However, these studies utilized *C. jejuni* strains from patients with enteritis that were not known to induce relevant antiganglioside responses. Nevertheless, exacerbated inflammatory responses in limited-flora SCID mice (Chang and Miller, 2006) and vancomycin treated Sigrr$^{-/-}$ mice (Stahl et al., 2014), taken together with our results in/ cefoperazone treated IL-10$^{-/-}$ mice, indicate that *C. jejuni*-mediated gastrointestinal inflammation is a multifactorial disease process mediated by both host microbiota and host genetics. In earlier work in this model using *C. jejuni* 11168 from a patient with enteritis, we found that dendritic cells from C57BL/6 IL-10$^{-/-}$ mice undergo activation and induce Th1-effector cell responses against *C. jejuni* (Rathinam et al., 2008). *C. jejuni* infected BM-DCs induced high level IFNγ production from CD4^{+}T cells indicating Th1 polarization. Furthermore, this activation involved cooperative signaling through Toll-Like Receptor 4 (TLR4)-MyD88 and TLR4-TRIF axes (Rathinam et al., 2009). The importance of TLR4 signaling with upregulation of Th1/Th17 cytokines in driving *C. jejuni* colitis was definitively confirmed by Stahl and colleagues in the Sigrr$^{-/-}$ mouse model although once again they used *C. jejuni* 81-176 that was isolated from a patient with gastroenteritis (Stahl et al., 2014).

Presumably, depletion of microorganisms that provide *C. jejuni* colonization resistance were eliminated by antibiotic treatment. Host genetics also play a role in *C. jejuni*-mediated inflammation. As Stahl et al. (2014) demonstrated, antibiotic depletion of gut microbiota enhanced susceptibility to *C. jejuni* colonization in C57BL/6 mice, but genetic manipulation— depletion of the single immunoglobulin interleukin-1 receptor-related protein (SIGIRR$^{-/-}$) in addition to antibiotic treatment—was required for severe enteric disease (Stahl et al., 2014). Similarly, decreased diversity of the intestinal microbiota present in limited flora (LF) mice diminished *C. jejuni* colonization resistance while only *C. jejuni* infected LF severe combined immune deficient mice (SCID) were susceptible to enteric disease (Chang and Miller, 2006).

Previously, we demonstrated that C57BL/6 IL-10$^{-/-}$ mice displayed contrasting immune responses meditating colitis and autoimmunity following *C. jejuni* infection (Malik et al., 2014). A *C. jejuni* 11168 isolate from a patient with colitis elicited severe Type1/17-dependent colitis in mice while three isolates (HB93-13, 260.94, CF93-6) from GBS patients elicited mild or no colitis and Type 2 cell mediated responses. To investigate how antibiotic depleted gut microbiota affects *C. jejuni*-mediated autoimmunity, we used the established mouse model of *C. jejuni* colitis C57BL/6 IL-10$^{-/-}$ (Malik et al., 2014; Mansfield et al., 2007) and treated the mice with cefoperazone (CPZ), a broad-spectrum antibiotic that has been shown to significantly deplete the murine microbiota (Antonopoulos et al., 2009; Nagalingam et al., 2013; Theriot et al., 2014; Yin et al., 2015). All *C. jejuni* strains used were resistant to cefoperazone as a result of the presence of the multidrug efflux pump *cmeABC* (Guo et al., 2010; Lin et al., 2002).

4. Results

Results from the three experiments are organized by the condition assessed or the assay performed so comparisons can be made. Experimental designs are shown in Table 1. In all experiments, mice received either sterile drinking water or 0.5 mg/mL CPZ in sterile drinking water for 7 days followed by oral gavage with one of three *C. jejuni* GBS patient strains or tryptone soy broth (the vehicle); antibiotic treatment was initiated one week prior to *C. jejuni* inoculation and continued for the entire duration of the experiment. Using established assays, we measured *C. jejuni* colonization, histopathological changes in the gut, and anti-*C. jejuni*- and anti-ganglioside antibodies in plasma collected from all experimental mice following sacrifice and compared them to controls. In one experiment, we measured neurological dysfunction.

4.1. Screening for enteric pathogens

To determine if mice were positive for enteric pathogens that could contribute to inflammatory responses we screened fecal samples from all experimental mice for *Campylobacter* spp.(Linton et al., 1996), *Helicobacter* spp.(Riley et al., 1996), *Enterococcus faecalis* (Dutka-Malen et al., 1995), and *Citrobacter rodentium* (McKeel et al., 2002). Mice were negative in all cases with the exception of *Campylobacter* spp. in experimentally inoculated mice.

4.2. Assessment of disease indicators

4.2.1. Survivorship

To compare the time to humane endpoint in all experimental mice we recorded the number of days post-inoculation until mice required sacrifice due to humane endpoints or until the scheduled euthanasia and necropsy at 5- or 7-weeks PI. In all cases mice were sacrificed if severe disease was detected using a standardized scoring sheet (see Methods). In the pilot experiment, one mouse in the 260.94 + CPZ group reached its humane endpoint prior to 5 weeks (Fig. 1A). In experiment 1 at least 40% of the mice in 260.94 + H_2O, 260.94 + CPZ, D8942 + H_2O, and D8942 + CPZ mice were sacrificed prior to 5 weeks PI because they reached the humane endpoint (Fig. 1B). In experiment 2 a single HB93–13 + H_2O mouse and 4 HB93–13 + CPZ mice reached the humane endpoint prior to 7 weeks PI (Fig. 1C).

4.2.2. Weight loss after C. jejuni HB93-13 infection

Mice were weighed at the time of sacrifice to investigate if *C. jejuni* inoculation resulted in disparity in final weight compared to controls. In the pilot experiment, no differences in weight were detected (Fig. 1D). Antibiotic treatment did not result in a disparity in weight gain in 260.94 or D8942 infected mice (Fig. 1E); however, HB93-13 infected, CPZ-treated mice gained significantly less weight than

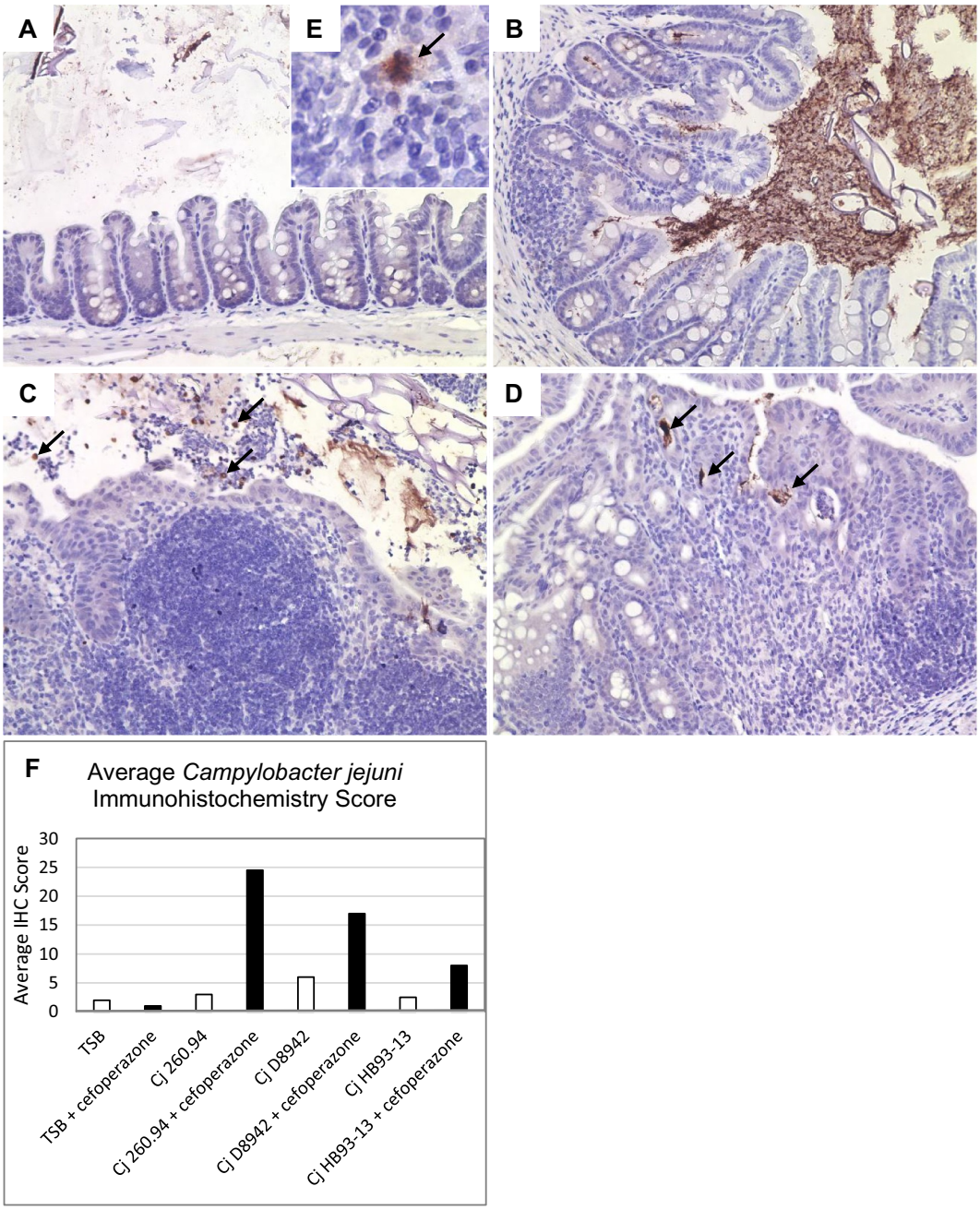

Fig. 2. Shows immunohistochemical staining for *Campylobacter jejuni* in mouse ileocecocolic tissues. Panel A is from a mouse given tryptone soya broth alone. Panel B was from a mouse given *C. jejuni* HB-93-13 with no antibiotic that shows staining associated with the contents, crypts and epithelial surface. Panel C is from a mouse given *C. jejuni* 260.94 and cefoperazone that show severe inflammation and staining associated with neutrophils in the exudate at the villus tip (arrows). Panel D is from the same mouse as C but shows staining associated with crypt abscesses (arrows). Inset E is from a mouse given *C. jejuni* D8942 and cefoperazone and shows the ileocecocolic lymph node draining the proximal colon. The arrow indicates a phagocytic cell with intracytoplasmic staining. Panel F shows the average *C. jejuni* specific immunohistochemical scores for the ileocecocolic junctions of mice from all groups. White bars indicate the treatment and sterile water given ad libitum; black bars indicate the treatment and cefoperazone in water given ad libitum.

uninfected-CPZ treated mice (Fig. 1F).

4.2.3. Mice treated with antibiotics had gastrointestinal tract gross pathological changes

During necropsy we evaluated gross pathologic changes in the cecum, colon and lymph nodes to determine if antibiotic treatment exacerbated pathology in infected mice. Inflammation of the cecum or colon; enlargement of lymph nodes or bloody feces were observed at necropsy and scored in a t ranked system (see Methods). In the pilot experiment, 3 of 4 260.94 + CPZ mice had gastrointestinal gross pathological changes while 1 of 4 260.94 + H_2O mice had GI gross pathological changes (Fig. 1G). To determine if enhanced inflammatory

and autoimmune responses (see below) in antibiotic treated mice were strain dependent, C57BL/6 IL-10$^{-/-}$ mice were inoculated with *C. jejuni* 260.94, D8942 or HB93-13 in one of two subsequent experiments. In experiments 1 and 2, gastrointestinal pathological changes could be detected by visual inspection in all infected + CPZ mice, infected with any *C. jejuni* strain (Fig. 1H and I). In Experiment 1, three of four 260.94 + CPZ mice had grade 2 pathology and one had grade 3 (Fig. 1H). In contrast, only one 260.94 + H_2O mouse had grade 2 pathology, and none had grade 3 (Fig. 1H). Three of four D8942 + CPZ and 3 of 4 D8942 + H_2O mice had grade 2 pathology (Fig. 2C). In experiment 2, a single mouse in both the uninfected + H_2O mouse and uninfected + CPZ showed gross pathological changes (Fig. 1I). In Experiment 2, gross pathological changes were similar in HB93-13 + H_2O and HB93-13 + CPZ mice except that all CPZ treated mice had lesions (Fig. 1I).

4.2.4. Antibiotic treatment depleted the microbiota and enhanced C. jejuni colonization in the cecal and colon contents

To determine if cefoperazone depleted the gut microbiota we used PCR to amplify the V3 region of the 16S rRNA gene in DNA isolated from the feces of experimental mice. The V3 region could be amplified from feces of uninfected + H_2O mice but not feces of uninfected + CPZ mice, confirming depletion of gut microbiota. To compare the level of *C. jejuni* colonization in the colon and cecum of experimentally inoculated mice, we streaked portions of both organs on TSA-CVA plates and analyzed *C. jejuni* levels using a semi-quantitative scoring system (Mansfield et al., 2007). In the pilot experiment, 3 of 4*C. jejuni* 260.94 + CPZ mice were culture positive in either the cecum or the colon or both compared to 1 of 5*C. jejuni* 260.94 + H_2O mice, indicating increased colonization of CPZ-treated mice (Fig. 1J). In experiment 1, 2 of 4 260.94 + H_2O and 4 of 5 260.94 + CPZ mice were culture positive at necropsy (Fig. 1K). All mice infected with *C. jejuni* D8942 were culture positive at necropsy (Fig. 1K). In experiment 2, 1 of 8 HB93–13 + H_2O mice compared to 7 of 7 HB93-13 + CPZ mice were culture positive (Fig. 1L). All control mice were negative by culture and *C. jejuni* specific PCR.

4.2.5. Antibiotic treatment of C. jejuni infected mice was associated with increased amounts of immunohistochemical staining and shifting of location of staining to deeper gut tissues and draining lymph nodes

To determine whether the *C. jejuni* GBS patient strains might be capable of invading tissues of the ICCJ and to determine the location of the organism in these tissues, IHC staining of paraffin embedded tissue was performed using a commercial *C. jejuni* specific antiserum. Results appear in Fig. 2. Sections from all mice in the TSB sham inoculated controls and cefoperazone alone treatment groups had no evidence of *C. jejuni* specific staining in any tissues, while mice in the *C. jejuni* infected groups all had staining associated with the contents and intestinal crypts. However, the degree of staining and location in tissues varied depending upon the infecting strain and whether antibiotic treatment was administered. Mice given all three *C. jejuni* strains had organism in the contents, mucus, crypts and adherent to the apical epithelium. Infected mice given antibiotics had organisms in these sites as well as within the paracellular junctions of the epithelium, at the basolateral surface of the epithelium, intracellular within the lamina propria and submucosa, and within cells of the draining lymph nodes. We found that the higher the IHC score the greater the amount of staining and the greater the number of deeper tissue sites demonstrated *C. jejuni* specific staining. Deep gut and lymphoid tissues from mice infected with *C. jejuni* 260.94 had the highest scores indicating greater tissue invasion and dispersal to draining lymphoid tissue. These mice also had significant staining associated with crypt abscesses and effacing lesions of the GI tract, while antibiotic treated infected mice given HB93-13 and D8942 had less staining in these sites and fewer lesions of this type. Panel F shows the average IHC scores for each group demonstrating that only *C. jejuni* infected and antibiotic treated groups had high scores and involvement of deeper tissues.

4.2.6. Neurological phenotyping test results

In Experiment 2, we videotaped mice weekly and evaluated the videotapes for signs of six behavioral/neurological deficits, including tail suspension test/spasticity, clasping reflex, movement in the open field test, rearing, gait abnormality, and respiratory effort (Hatzipetros et al., 2015). Each character was scored as “present” or absent”. Thus, the range of neurologic scores was 1–6 events. Mice in all groups were judged to have no phenotypic signs of neurological disease at the start of the experiment (Fig. 3; Fig. 4). Mice infected with *C. jejuni* strains from GBS patients exhibited some neurological signs (Fig. 3; Fig. 4). The percentage of mice showing neurological signs was greater in infected mice given CPZ at later time points post infection. Infected mice, and especially those treated with CPZ, showed decreased ambulation and numbers of rears, which was not evident until 5 weeks after infection. The percent of mice with normal stride length was significantly lower in infected CPZ treated mice at 7 weeks post infection. Mice in this group also showed increased spasticity and respiratory effort. These mice spent most of their time in one spot in the open field chamber and exhibited repeated deep excursions of their thoracic cavities despite the absence of visual or auditory stimulation. However, despite this increased respiratory effort, these mice had adequate capillary refill times.

In Fig. 4, a heat map diagram shows the number of neurologic signs scored at weekly intervals after sham inoculation or infection with *C. jejuni* strain HB93-13 in Experiment 2 and the correlation of neurologic signs with colitis scores. Although a few events were noted in the uninfected sham inoculated group, a significant number of mice in *C. jejuni* HB93-13 group and the infected and CPZ treated group had high scores beginning at Day 14 post infection and extending up to Day 49 post infection (Fig. 4). All mice in the *C. jejuni* HB93-13-infected, CPZ-treated group had severe colitis based on histopathologic scoring of the ileocecocolic junction. Seven of eight of these mice showed some neurologic signs. However, 4 of 8 mice required euthanasia due to reaching a humane endpoint necessitated by signs of GI disease or neurological disease. Yet all mice in the *C. jejuni* HB93-13 alone group had neurologic signs, and 5 of these had high neurologic scores.

4.3. Assessment of innate and adaptive immunological responses

4.3.1. Assessing inflammatory gastrointestinal lesions and colonic T cell populations

4.3.1.1. Antibiotic treatment elicited severe ileocecal typhlocolitis in all infected mice even those given C. jejuni strains that heretofore caused no enteric lesions. We examined hematoxylin and eosin stained sections of the ICCJ of experimentally inoculated mice for inflammation and other pathologic changes. Tissues represent all experimentally inoculated mice colonized for 5 weeks (pilot and experiment 1), 7 weeks (experiment 2) or humane endpoint with *C. jejuni* 260.94, D8942, and HB93-13, and from sham-inoculated controls. Histologic scores were assigned using a standardized scoring system with a range of 0 to 40 (Mansfield et al., 2007). In all, two control mice showed inflammation in the ICCJ (Fig. 5A and C) consistent with previous reports of spontaneous colitis in C57BL/6 IL-10$^{-/-}$ mice in response to stimulation by microbiota (Bristol et al., 2000). Mice with spontaneous colitis were negative by PCR for enteric pathogens (see Methods) including *C. jejuni* assayed both by culture and by *gyr*A PCR (Wilson

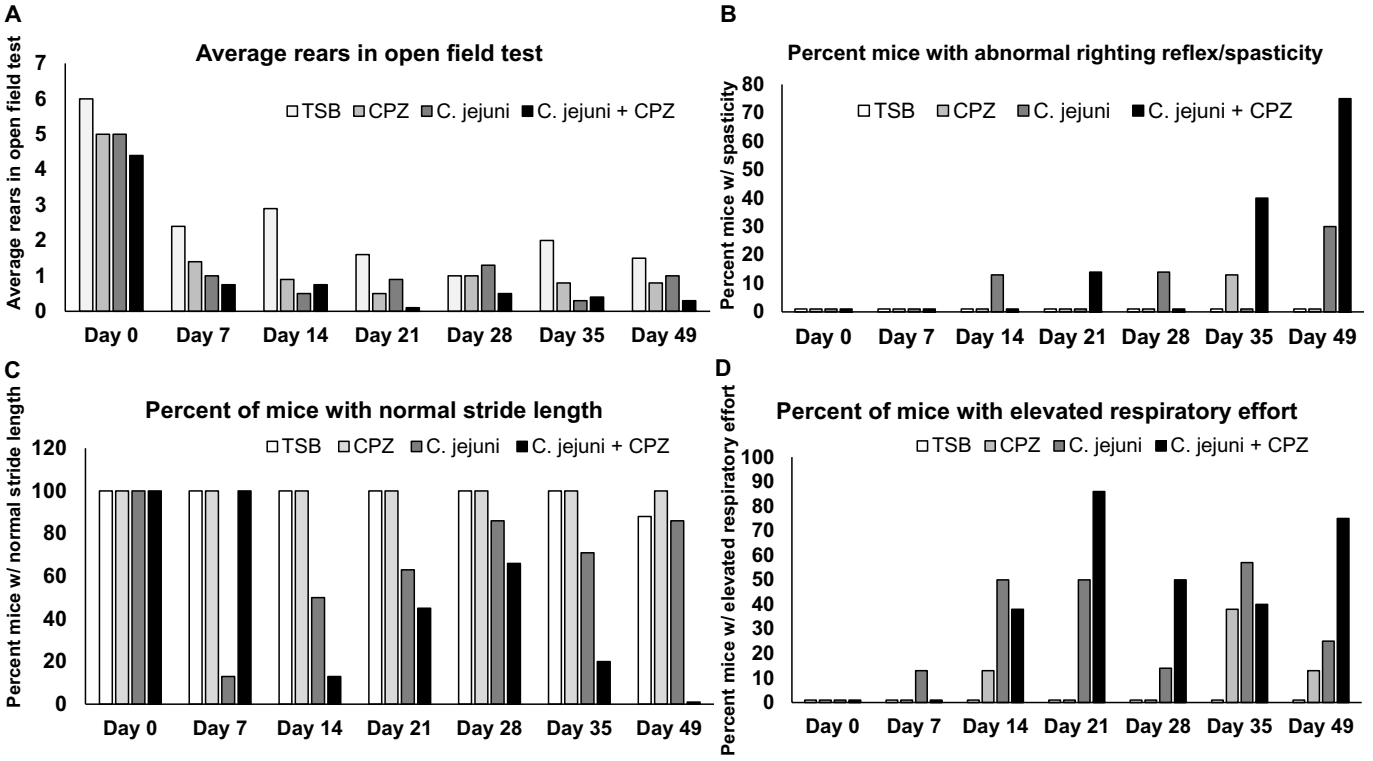

Fig. 3. Neurologic phenotyping assessments by open field test. A) Average rears in open field test, B) percent of mice with abnormal righting reflex/spasticity, C) percent of mice with a normal stride length, and D) percent of mice with elevated respiratory effort. Data shown was calculated from open field test videos of mice in the four experimental groups. All assessments were made by scoring videos that were blinded for mouse identity and group assignment.

et al., 2000).

In the pilot experiment and in experiment 1, there was a strong trend to high histologic scores in the ICCJ in *C. jejuni* infected mice given antibiotics compared to the uninfected control group, but statistically significant differences were not detected (Fig. 5A–C). In the pilot experiment, 3 of 4 260.94 + CPZ mice had histologic scores of > 30 indicating severe tissue damage (Fig. 5A). In experiment 1, these high histologic scores in *C. jejuni* infected mice given CPZ were also severe with all mice achieving the highest grade of 3 compared to uninfected controls that were all grade 1, which are considered normal (Fig. 5B). In experiment 1, the median scores for ICCJ histopathology of mice in the infected groups were as follows: 3 for 260.94 + H_2O, 36 for 260.94 + CPZ, 12 for D8942 + H_2O, and 35.5 for D8942 + CPZ (Fig. 5A–B). In experiment 2, histopathology scores were significantly increased in HB93–13 + CPZ mice compared to uninfected, antibiotic treated and untreated controls (Fig. 5C). A single mouse in both the uninfected + H_2O and HB93–13 + H_2O groups in experiment 2 had a score 27 and 36 respectively (Fig. 5C).

When present, inflammation and tissue damage affected the colon and cecum but not the ileum. In general, except for the 2 mice with spontaneous colitis mentioned above, uninfected + H_2O mice did not show inflammation (Fig. 5D–F, 2×, 20×, 40×), and antibiotic treatment did not elicit pathological changes in the absence of *C. jejuni* (Fig. 5G–I, 2×, 20×, 40×). Infection with *C. jejuni* 260.94 alone did not elicit significant inflammation, yet the lesions seen consisted of neutrophils and mononuclear cells in the lumen and epithelium of the cecum and colon (Fig. 5J–L 2×, 20×, 40×). In stark contrast, antibiotic treatment instigated severe inflammation in the cecum and colon of mice infected with 260.94. These lesions included increased neutrophils and mononuclear cells in the lumen, epithelium, lamina propria, and submucosa, excess mucus in the lumen, epithelial effacing lesions and ulcerations, marked crypt hyperplasia, increased neutrophils in crypts, marked increases in lamina propria cellularity consisting primarily of diffusely distributed mononuclear cells, inflamed myenteric plexus, diffuse mononuclear submucosal inflammation, and submucosal edema and vasculitis (Fig. 5M–O). Infection with D8942 elicited mild inflammation associated primarily with neutrophilic and mononuclear cells in the lumen and epithelium (Fig. 5P, 20×), which was exacerbated by antibiotic treatment (Fig. 3–5Q, 20×) in a manner consistent with that seen in mice given 260.94 + CPZ and HB93-13 + CPZ mice (Fig. 5R, 20×).

4.3.1.2. Antibiotic treatment enhanced T cell responses in infected, antibiotic treated mice. Based on our previous report showing that T-cells are required for colitis in C57BL/6 IL-10$^{-/-}$ mice (Malik et al., 2014), we isolated colonic lamina propria leukocytes and sorted them by flow cytometry to determine if expected T cell mediated inflammation in *C. jejuni* infected mice was exacerbated by antibiotic treatment. In the pilot experiment, 260.94 + CPZ mice exhibited significant increases in total T cells ($CD19^-$ $CD3^+$)(Figs. 4–6A), T_H cells ($CD3^+CD19^-CD4^+$)(Figs. 4–6D), T_H1 cells ($CD3^+CD19^-CD4^+IFN\gamma^+$)(Figs. 4–6G), and T_H2 cells ($CD3^+CD19^-CD4^+IL4^+$)(Figs. 4–6J) compared to compared to uninfected mice not given antibiotic. In experiment 1, 260.94 + CPZ mice had a significant increase in total T cells ($CD3^+$ $CD19^-$) (Fig. 4–6B), total T helper cells ($CD3^+$ $CD19^-$ $CD4^+$) (Fig. 4–6E), and T_H1 cells ($CD3^+$ $CD19^-$ $CD4^+$ $IFN\gamma^+$)(Figs. 4–6H) compared to uninfected mice given CPZ. This enhanced T_H1 response was not

Mouse Number	Sex	Inoculum	CPZ Tx	Neurological phenotyping score, days post infection							Colitis Score
				Day 0	Day 7	Day 14	Day 21	Day 28	Day 35	Day 49	
9234	F	TSB		0	0	0	0	0	0	0	0
9258	F	TSB		0	0	0	1	0	0	0	0
9273	F	TSB		0	0	0	0	0	0	0	0
9269	F	TSB		0	0	0	0	0	1	0	0
9228	M	TSB		0	0	0	1	0	0	0	0
9254	M	TSB		0	0	0	1	0	0	0	0
9261	M	TSB		0	0	0	0	0	0	0	0
9267	M	TSB		0	0	0	0	0	0	2	0
9270	F	TSB	CPZ	0	0	1	1	0	0	1	0
9235	F	TSB	CPZ	0	0	0	1	1	0	0	0
9259	F	TSB	CPZ	0	0	0	0	0	1	1	0
9274	F	TSB	CPZ	0	0	0	0	1	1	0	0
9229	M	TSB	CPZ	0	0	2	1	0	0	1	0
9255	M	TSB	CPZ	0	0	0	0	1	0	2	0
9262	M	TSB	CPZ	0	0	0	1	1	2	1	0
9268	M	TSB	CPZ	1	0	0	0	0	1	1	0
9271	F	HB93-13		0	0	1	0	0	0	0	0
9232	F	HB93-13		0	0	2	1	2	3	1	0
9256	F	HB93-13		0	0	1	1	1	1	1	0
9275	F	HB93-13		0	0	5	2	1	2	3	0
9264	F	HB93-13		0	2	4	3				1
9230	M	HB93-13		0	0	1	0	1	2	0	0
9276	M	HB93-13		0	2	3	2	2	2	3	0
9263	M	HB93-13		0	0	0	3	1	2	5	0
9257	F	HB93-13	CPZ	0	1	2	6	3	3	3	1
9265	F	HB93-13	CPZ	0	1	0	1	0			1
9272	F	HB93-13	CPZ	0	0	1	2				2
9233	F	HB93-13	CPZ	0	1	2	4	1	1		2
9231	M	HB93-13	CPZ	0	0	0	3	1	2	3	2
9277	M	HB93-13	CPZ	0	1	1	2	2	3	4	2
9260	M	HB93-13	CPZ	0	0	0	2	3	4	4	2

Fig. 4. Heatmap summary of neurological phenotyping and colitis outcomes for Experiment 2. Heatmap shows the open field test weekly phenotyping for all mice in the four treatment groups including trypticase soya broth (TSB) sham inoculated, TSB sham inoculated given cefoperazone (CPZ) antibiotic, *C. jejuni* HB93-13 infected and *C. jejuni* HB93-13 infected given CPZ. The number of abnormal findings is given for each mouse at each phenotyping day and scores range from 1 in pale blue through darker shades of blue to the darkest at 6 abnormal findings. Gray shading indicates that mouse was humanely euthanized and did not continue beyond first date indicated. Colitis scores are given as ranks 0 = normal, 1 = mild colitis (pale orange), and 2 = severe colitis (dark orange). (For interpretation of the references to color in this figure legend, the reader is referred to the web version of this article.)

associated with a statistically significant change in T_H2 cells ($CD3^+$ $CD4^+$ $IL4^+$) (Figs. 4–6K), indicating that antibiotic administration was associated with a mixed T_H1/T_H2 response in *C. jejuni* 260.94 infected mice (Figs. 4–6E and H). These results were specific to strain 260.94; strain D8942 did not produce significant changes in T cell populations. In experiment 2, there was a significant increase in total T-cells (Figs. 4–6C) and T helper cells (Fig. 6F) in HB93–13 + CPZ mice compared to uninfected mice not given antibiotic; HB93–13 + CPZ mice had significantly more total T helper cells than HB93–13 infected mice not given antibiotic. However, T_H1 and T_H2 cell numbers were not statistically significantly different in HB93–13 + H_2O or HB93–13 + CPZ compared to controls (Fig. 6I and L) at 7 weeks PI.

Next, we evaluated the frequency of T_H cells and T_H1 and T_H2 to determine if a shift in T_H1 and T_H2 cells was apparent. In the pilot experiment and experiment 2, the frequency of Th cells was significantly higher in the *C. jejuni* infected and antibiotic treated groups (Fig. 6M and O). In the pilot experiment, T_H1 cells were elevated compared to controls (i.e. uninfected + H_2O) and T_H2 cells diminished compared to 260.94 + H_2O (Fig. 6P and S). Similarly, in experiment 1, the frequency of T_H1 cells was elevated in 260.94 + CPZ and D8942 + CPZ mice compared to uninfected + CPZ mice (Fig. 6Q). In addition, T_H2 cells were diminished in 260.94 + CPZ mice but not D8942 + CPZ mice (Fig. 6T). No differences were detected in the frequency of T_H1 or T_H2 cells in experiment 2, 7 weeks post infection

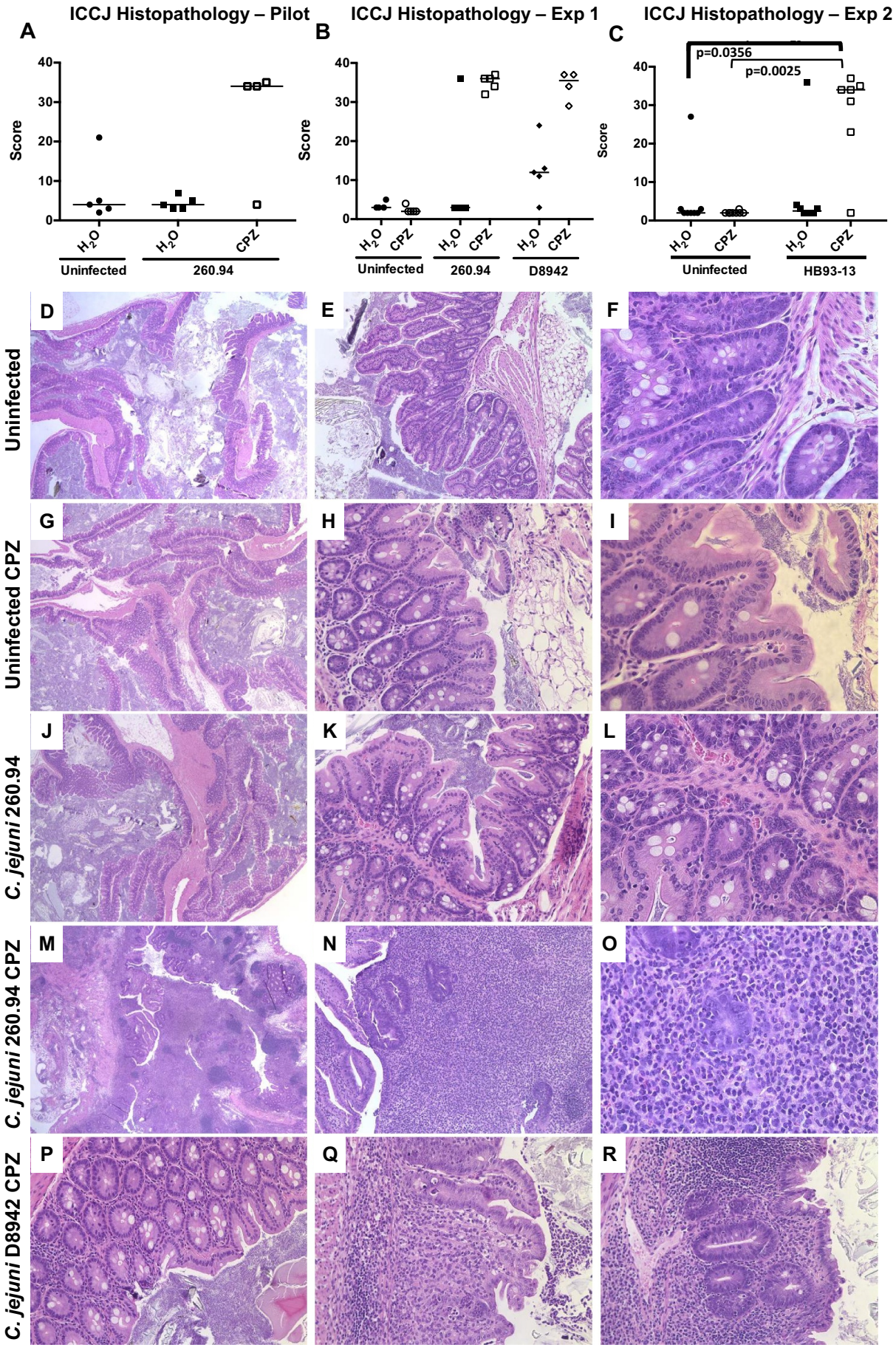

(caption on next page)

Fig. 5. Cefoperazone treatment enhances ileocecocolic lesions. Ileocecocolic junctions (ICCJ) were collected at necropsy and fixed in 10% formalin. Sections were stained with hematoxylin and eosin (H and E), and based on inflammation and tissue damage received a score ranging from 0 to 41. Summarized results appear as follows: A) pilot, B) experiment 1, and C) experiment 2. Symbols represent the score of 4–8 animals per group and bars represent the median. Data were considered statistically significant if $p < 0.05$ after correction for multiple comparisons. Representative sections are shown for the following groups: D) uninfected + H_2O, 2X, E) uninfected + H_2O, 20X, F) uninfected + H_2O, 40X, G) uninfected + CPZ, 2X, H) uninfected + CPZ, 20X, I) uninfected + CPZ, 40X, J) 260.94 + H_2O, 2X, K) 260.94 + H_2O, 20X, L) 260.94 + H_2O, 40X, M) 260.94 + CPZ, 2X, N) 260.94 + CPZ, 20X, O) 260.94 + CPZ, 40X, P) D8942 + H_2O 20X, Q) D8942 + CPZ 20X, and R) HB93-13 + CPZ,20X are H and E stained ICCJ sections at various magnifications.

(Fig. 6R and U).

4.3.2. Antibody isotype production and macrophage infiltration of dorsal root ganglia and sciatic nerve

Type 1, 2, and 17 cytokines are known to modulate B cell class switching; IFNγ (T_H1) has been associated with IgG2c and IgG3 responses, while IL-4 (T_H2) has been associated with IgE and IgG1 responses, and IL-17 (T_H17) with IgG2b responses (Bai et al., 2008; Germann et al., 1995; Zhang et al., 2013).

4.3.2.1. T_H1 associated antibody responses. To determine if T_H1-associated IgG2c antibody responses were elicited by *C. jejuni* infection and exacerbated by antibiotic treatment we measured IgG2c type antibodies in the plasma of experimental mice by indirect ELISA. In the pilot experiment, a significant increase in anti-*Campylobacter* IgG2c antibodies was detected between untreated + H_2O and 260.94 + CPZ groups ($p = 0.171$) (data not shown). In experiment 1, antibiotic treatment elicited an anti-*Campylobacter* IgG2c response in 260.94 infected but not in D8942 infected mice (Fig. 7A). In experiment 2, anti-*Campylobacter* IgG2c responses were modest but elevated in the HB93-13 + H_2O and HB93-13 + CPZ groups (Fig. 7B).

Next, to determine if T_H1-associated IgG2c antibodies were cross-reactive with peripheral nerve gangliosides GM1 and GD1a, we performed indirect IgG2c anti-ganglioside ELISAs. Although anti-*C. jejuni* IgG2c antibodies were only elevated in 260.94+ CPZ mice in experiment 1, IgG2c anti-ganglioside antibodies cross reactive with both GM1 (Fig. 7C) and GD1a (Fig. 7E) were increased in both 260.94 + CPZ and D8942 + CPZ groups compared to uninfected + CPZ mice. When comparing this response in mice given *C. jejuni* strain HB93-13 in experiment 2, GM1 and GD1a antibodies were elevated in HB93-13+ CPZ compared to both untreated + CPZ and untreated + H_2O mice (Fig. 7D and F).

4.3.2.2. T_H17 associated antibody responses. We next analyzed the levels of T_H17-associated IgG2b antibodies reactive with *C. jejuni* and gangliosides GM1 and GD1a (Figs. A-F). In the pilot experiment, antibiotic treatment resulted in significant increases in anti-*C. jejuni* IgG2b in 260.94 + CPZ compared to uninfected + H_2O ($p = 0.0040$) (data not shown). In experiment 1, significant differences were detected in anti-*C. jejuni* IgG2b antibody levels between uninfected + H_20 and 260.94 + CPZ but not D8942 + CPZ groups (Fig. 8A). In contrast, in experiment 2, anti-*C. jejuni* Ig2b antibodies were elicited by infection alone and exacerbated by antibiotic treatment (Fig. 8B). Interestingly, neither *C. jejuni* 260.94 nor D8942 alone elicited significant IgG2b anti-ganglioside antibodies (Fig. 8C and D); however, consistent with the anti-*C. jejuni* IgG2b responses produced by these two *C. jejuni* strains, infection with HB93–13 also elicited anti-GD1a IgG2b antibodies which were exacerbated by antibiotic treatment compared to uninfected + H_2O group (Fig. 8F).

In experiment 2, in both infected groups, neurologic scores correlated with elevated anti-GM1 IgG1 antibodies. Interestingly in the CPZ alone treatment group, two mice had similar antiganglioside antibodies, and all had slight evidence of neurologic signs suggesting that bacteria within the microbiota may elicit antiganglioside antibodies.

4.3.2.3. T_H2 associated antibody responses. Finally, we assessed the abundance of T_H2 associated IgG1 anti-*C. jejuni* and anti-ganglioside antibodies in the same manner described for other antibody types (Fig. 9 7 A-I). We did not detect a significant increase in anti-*Campylobacter* or anti-ganglioside antibodies in either the pilot experiment (*C. jejuni* 260.94) or experiment 1 (*C. jejuni* 260.94 and D8942) (Fig. 9A, B, D, E, G, H). In contrast, in experiment 2, infection with *C. jejuni* HB93-13 elicited both anti-*Campylobacter* and anti-ganglioside antibodies compared to uninfected, non-antibiotic-treated controls. Furthermore, both the HB93-13 + H_2O and HB93-13 + CPZ groups had enhanced anti-GM1 IgG1 (Fig. 9F) but not anti-GD1a (Fig. 9I) antibody responses compared to the uninfected + H_2O group. These outcomes also suggest that these T_H2 associated responses are greater at 7 than 5 weeks post infection.

4.3.2.4. Assessing peripheral nerve lesions and macrophage infiltration in sciatic nerve and dorsal root ganglia by anti-F4/80 immunohistochemical staining. Finally, having detected anti-ganglioside antibodies in *C. jejuni* infected mice, we expected that infected + H_2O groups might display enhanced macrophage numbers in peripheral nerves and dorsal root ganglia compared to controls, and these lesions would be exacerbated in infected + CPZ groups. Table 2 shows all antiganglioside antibodies detected in mice in Experiments 1 and 2 and their correlation with macrophage numbers in peripheral nerves. Finally, high levels of F4/80 positively staining macrophages within the dorsal root ganglion and the sciatic nerves of these mice mainly correlated with *C. jejuni* HB93-13 infection with and without CPZ (Fig. 10).

Statistically significant increases in macrophage number were not detected in any group compared to the uninfected + H_2O groups, although there was a trend toward increased macrophage numbers on *C. jejuni* 260.94 infected mice given CPZ (Fig. 10A-D). Thereafter, antibody responses divided by class and ganglioside cross reactivity (i.e. GM1 or GD1a), corresponding to individual mice, were compared to macrophage counts in both the DRG and the SN, to determine if the presence of anti-ganglioside antibodies or of particular types of anti-ganglioside antibodies was correlated with increased macrophage count (Table 2). In experiment 1 this analysis revealed (1) that many of uninfected + CPZ mice had increased macrophage numbers compared to uninfected + H_2O group controls; (2) that macrophages were present in higher numbers in infected mice in experiment 1 and were generally located in the DRG; and (3) that increased macrophage number was not associated with the presence of any particular class of anti-ganglioside antibody. Notably, 1 of 4 mice in the 260.94 + H_2O group had increased macrophage numbers versus 5 of 5 mice in the 260.94 + CPZ group. In contrast, 4 of 5 D8942 + H_2O group mice had increased macrophages numbers in their DRG compared to only 1 of 4 D8942 + CPZ group mice. In experiment 2, no HB93-13-infected non-antibiotic-treated mice displayed increased macrophage numbers in the DRG; however, 3 of 7 HB93-13-infected, CPZ-treated mice did have elevated numbers of macrophage in the DRGs. Elevated macrophage numbers were infrequent in SN nerves of both treated and untreated

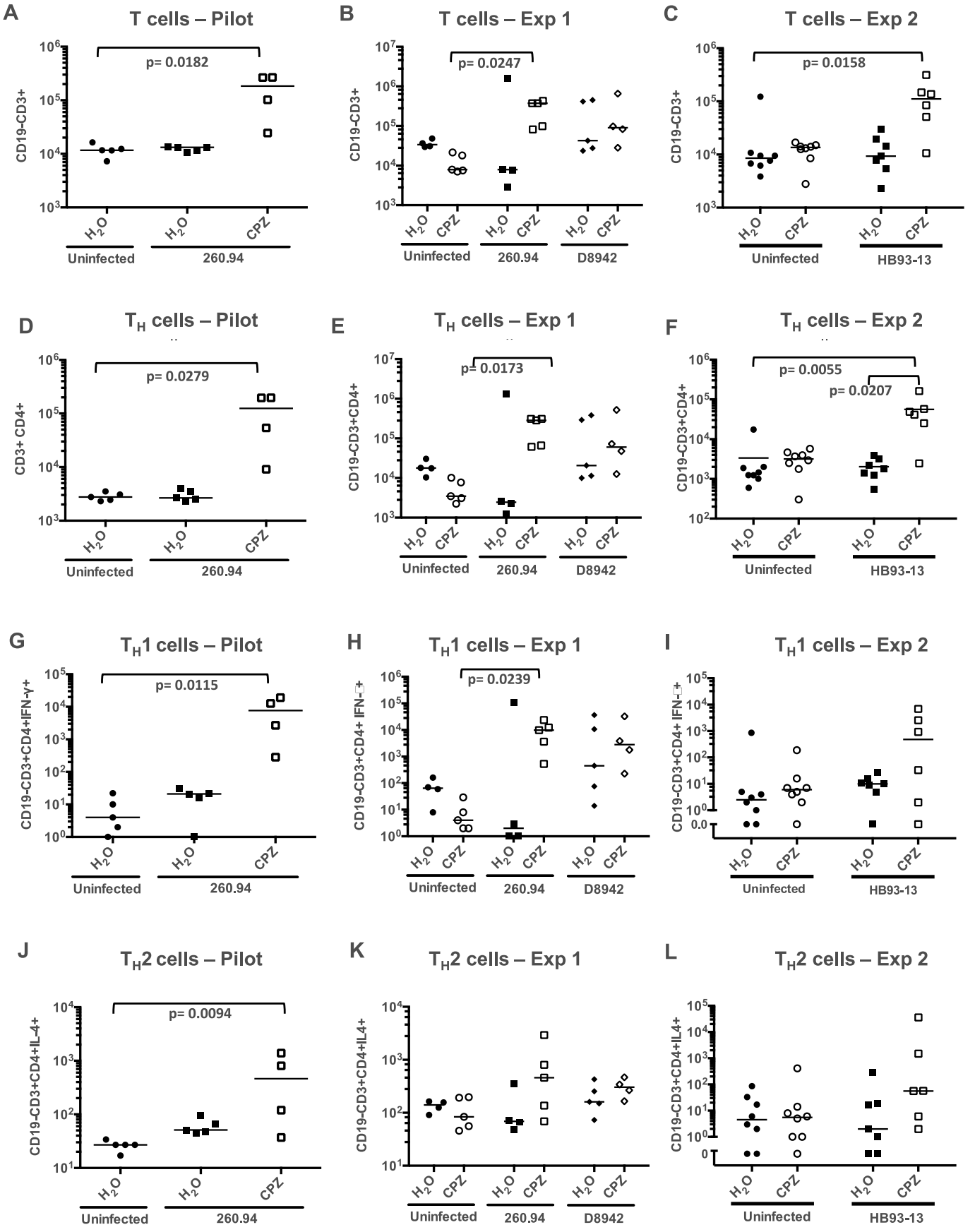

(caption on next page)

Fig. 6. Endpoint lamina propria leukocyte analysis via flow cytometry: Pilot experiment, Experiment 1 and Experiment 2. Colon leukocytes were isolated from C57BL/6 IL-10$^{-/-}$ mice at 5 weeks (pilot and experiment 1), 7 weeks (experiment 2), or humane endpoint and sorted by flow cytometry. Dead and dying cells were excluded based on forward and side scatter. All cells were gated on CD19^{-} CD3^{+} gate. Each symbol represents a single animal; bars represent medians with 4–5 mice per group (Pilot and experiment 1) or 6–8 mice per group (experiment 2); data were analyzed by the Kruskal-Wallis test on ranks with Dunn's post test and $p < 0.05$ was considered statistically significant. Panels A-L show numbers of cells detected. Panels A, D, G, J and M show data from the Pilot Experiment. Panels B, E, H, K, and N show data from Experiment 1. Panels C, F, I, L and O show data from Experiment 2. For each panel the Y axis and heading give the cell type evaluated. Panels M-U show the frequency of the specific cell type detected.

HB93-13 infected mice.

Fig. 10E shows a section of a DRG and Fig. 10F shows a section from a sciatic nerve of an uninfected mouse both showing little to no macrophages staining. Fig. 10G, shows a section of a DRG and Fig. 10H shows a section of a sciatic nerve both from a *C. jejuni* 260.94 infected mouse given CPZ with positively staining macrophages.

4.3.3. Summary of Experiment 2: putting it all together

Fig. 11 shows a summary of disease indicators and immunological data for each animal in Experiment 2. Color-coding for colitis scores and neurological phenotyping are the same as in Fig. 4. Colored cells in the remaining columns indicate values greater than the sum of the mean of the TSB only group plus twice the standard deviation of that group (given in the last row). The data indicate that microbiota depletion by antibiotic treatment exacerbated colitis due to *C. jejuni* HB93-13 infection compared to infected, non-antibiotic-treated controls. *C. jejuni* HB93-13 infection was associated with neurological deficits and elevated T_H2-associated IgG1 anti-*C. jejuni* and anti-ganglioside antibody levels in both antibiotic-treated and non-antibiotic-treated mice. It is interesting to note that 3 of 8 uninfected antibiotic-treated mice had elevated anti-ganglioside IgG1 responses; this result suggests that some members of the microbiota may carry ganglioside-like epitopes that are released by death of susceptible cells. Numbers of macrophage in dorsal root ganglia were only elevated in antibiotic treated, *C. jejuni*-infected mice. In general, increased enteritis was accompanied by increased immunological and histopathological evidence of GBS-like disease, and antibiotic depletion of the microbiota appeared to exacerbate this effect.

To develop a comprehensive view of the findings from Experiment 2 in the context of GBS, we assessed the combined manifestations of neurological disease by assigning a value of 1 to each of six parameters measured: 1) neurological phenotype (defined as a score ≥ 3 on at least one day post inoculation), 2) elevated anti-C. jejuni IgG1 levels, 3) elevated anti-ganglioside GM1 IgG1, 4) elevated anti-ganglioside GD1a IgG1, 5) elevated numbers of macrophage in the sciatic nerve, and 6) elevated numbers of macrophage in the dorsal root ganglia; these values were summed for each animal. Fig. 12 shows the distribution of these scores in the four treatment groups. Kruskal Wallis one-way ANOVA on ranks was significant for these data ($P = 0.0004$). Mann-Whitney pairwise comparisons that were significant after Bonferroni correction for multiple comparisons were non-antibiotic-treated TSB-inoculated mice versus non-antibiotic-treated HB93-13-inoculated mice ($P = 0.0055$), non-antibiotic-treated TSB-inoculated mice versus antibiotic-treated HB93-13-inoculated mice ($P = 0.0058$), and non-antibiotic-treated TSB-inoculated mice vs antibiotic-treated HB93-13- inoculated mice ($P = 0.0463$). No other pairwise comparisons were significant; the P value for the comparison of non-antibiotic-treated HB93-13-inoculated mice versus antibiotic-treated HB93-13-inoculated mice was 0.1257.

5. Discussion

Our group previously showed that Non-obese-diabetic (NOD) mice were susceptible to GBS when given *C. jejuni* from patients with this neurological disease (St Charles et al., 2017). Here we sought to explore the susceptibility of mice of a different genetic background where colitis but not GBS had been explored. Another goal was to explore the role of the microbiome in colitis and GBS outcomes in the simplest scenario where antibiotics decreased microbiome diversity. In these experiments, we took advantage of the intrinsic resistance to the broad spectrum antibiotic cefoperazone that is mediated in *C. jejuni* by a highly conserved multidrug efflux system, CmeABC (Guo et al., 2010; Lin et al., 2002). This resistance allowed *C. jejuni* to persist in the gut in the face of a treatment that removed most of the other members of the gut microbiota and allowed us to evaluate the role of the microbiota in *C. jejuni* enteritis and its neurological sequelae.

Antibiotic depletion of microbiota by CPZ increased *C. jejuni* colonization levels, the percentage of mice colonized and the distribution of the bacterium in the gastrointestinal tract although variation in these outcomes occurred based on the strain. Regardless of the *C. jejuni* load in infected mice, there was a dramatic increase in the number of animals colonized with HB93-13 and 260.94 in the cecum or colon when antibiotic treatment was given compared to untreated mice. Semi-quantitative culture of *C. jejuni* in cecum and colon showed increases in infected antibiotic treated mice compared to infected mice given only sterile water, yet, even without antibiotics colonization levels were high (data not shown). However, immuno-histochemical analysis showed darker staining, a greater area of staining and a greater depth of tissue staining in infected mice given the antibiotic. Antibiotic treatment also caused higher numbers of invasive *C. jejuni* that were found associated with the apical, basolateral and paracellular junctions of the epithelium and within cells of the lamina propria, submucosa and lymph nodes indicating increased invasion and translocation from the gut. Collectively these results indicate immune deficient hosts are made more vulnerable to *C. jejuni*-mediated-inflammation when microbiota are depleted as shown by antibiotic treatment. These results suggest that elimination of microbiota with antibiotic treatment removed commensal organisms responsible for *C. jejuni* colonization resistance and allows for increases in *C. jejuni* colonization. Antibiotic depletion of gut microbiota was the main factor in the manifestation of enhanced enteric disease although the severity of the enteritis was also dependent on the infecting strain of *C. jejuni*. Infected mice given CPZ had marked decreases in survivorship and increases in both gross and histopathologic scores in the colon. *C. jejuni* 260.94 produced the greatest *C. jejuni* positive immunohistochemical scores in the gut, indicating greater tissue invasion and dispersal to draining lymphoid tissue. These mice also had significant staining associated with crypt abscesses and effacing lesions of the GI tract, while antibiotic treated infected mice given HB93–13 and D8942 had less staining in these sites and fewer lesions of this type. Interestingly, antibiotic treatment drove severe colitis by *C. jejuni* strains isolated from GBS patients that had heretofore produced no or only mild colitis in this model, especially *C. jejuni* 260.94 (Malik et al., 2014).

We considered whether depletion of gut microbiota with a broad-spectrum antibiotic increased severity of GBS when *C. jejuni* infecting strains possess lipooligosaccharides resembling host gangliosides.

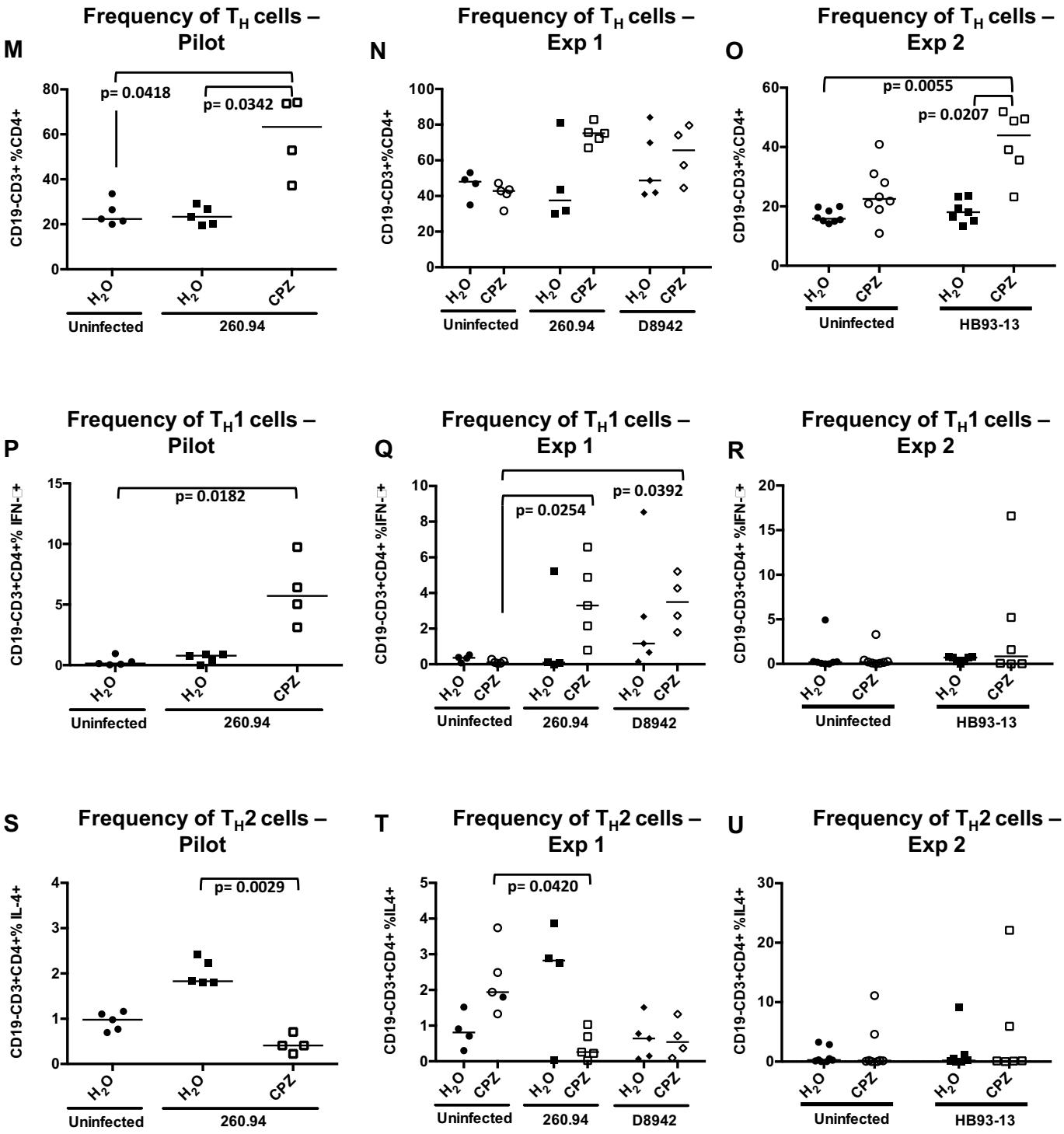

Fig. 6. (*continued*)

Although depletion of the microbiota has been shown to increase *C. jejuni* intestinal colonization (Chang and Miller, 2006; O'Loughlin et al., 2015b) no one has explored whether increased colonization levels result in increased anti-ganglioside antibodies. Our work provides the first evidence that antibiotic depletion of gut microbiota influences anti-ganglioside antibody responses and neurologic signs. There were more CPZ-treated, infected mice with antiganglioside antibodies than water-treated infected mice. Presence of anti-ganglioside antibodies in infected mice were correlated with an increase in the colonization levels of *C. jejuni* and in the number of mice with *C. jejuni* 260.94 and HB93-13 colon and cecum positive cultures at sacrifice. In a few infected mice the specific *C. jejuni* strain alone was sufficient to induce antiganglioside antibody production. Not all *C. jejuni* strains elicit antiganglioside autoantibodies. *C. jejuni* 11168 from a patient with

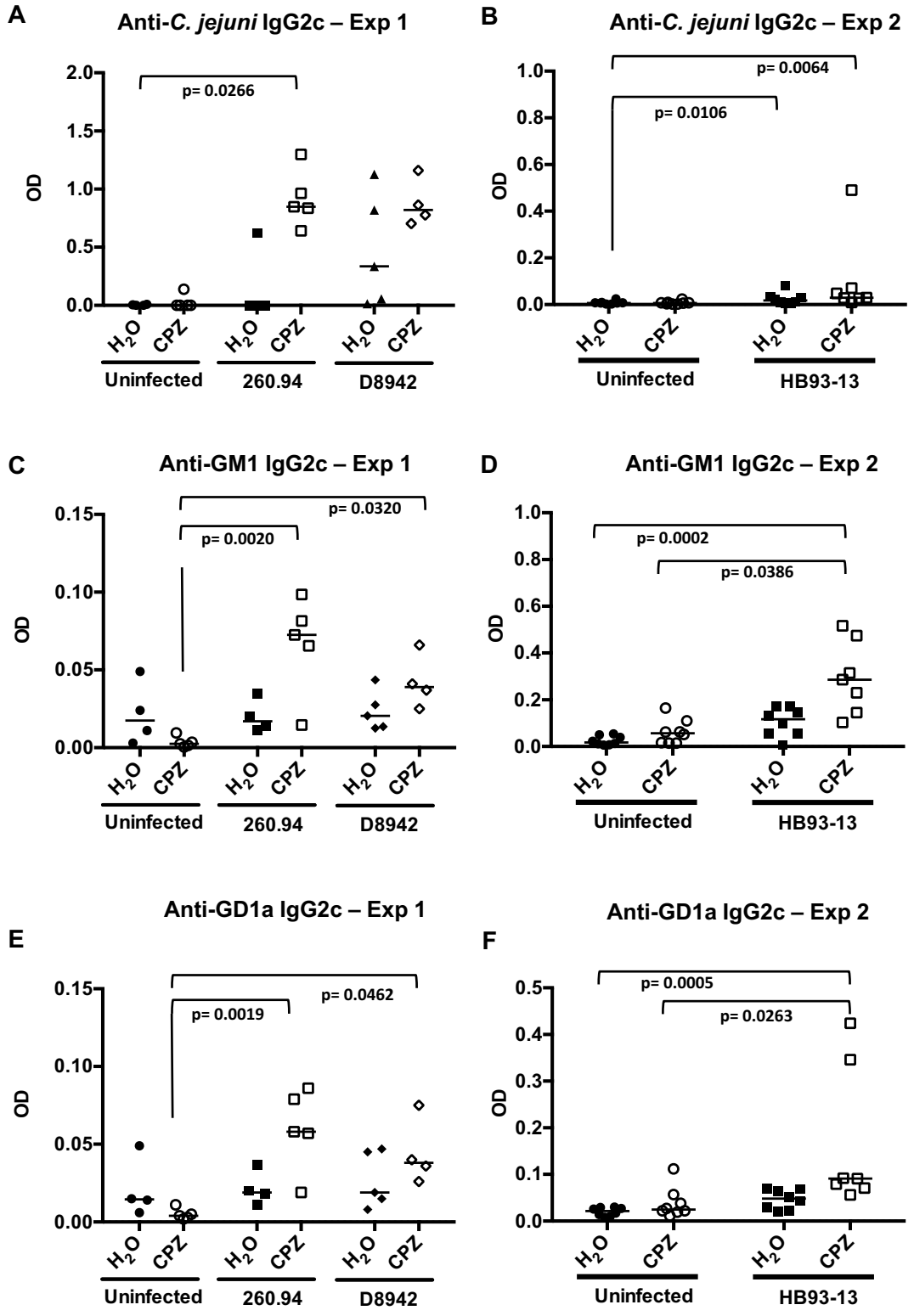

Fig. 7. Type 1 antibody responses were exacerbated by antibiotic treatment. Plasma antibodies reactive with gangliosides (GM1 and GD1a) and *C. jejuni* antigen were measured via indirect ELISA. Biotinylated goat anti-mouse secondary antibodies were used to determine IgG subclass. Each symbol represents a single animal; bars represent group means. Data represent 4–5 mice per group (Pilot and Experiment 1) or 6–8 mice (Experiment 2); and the means of 3 replicate wells per sample were analyzed by Kruskal-Wallis test on ranks with Dunn's post test and $p < 0.05$ was considered statistically significant.

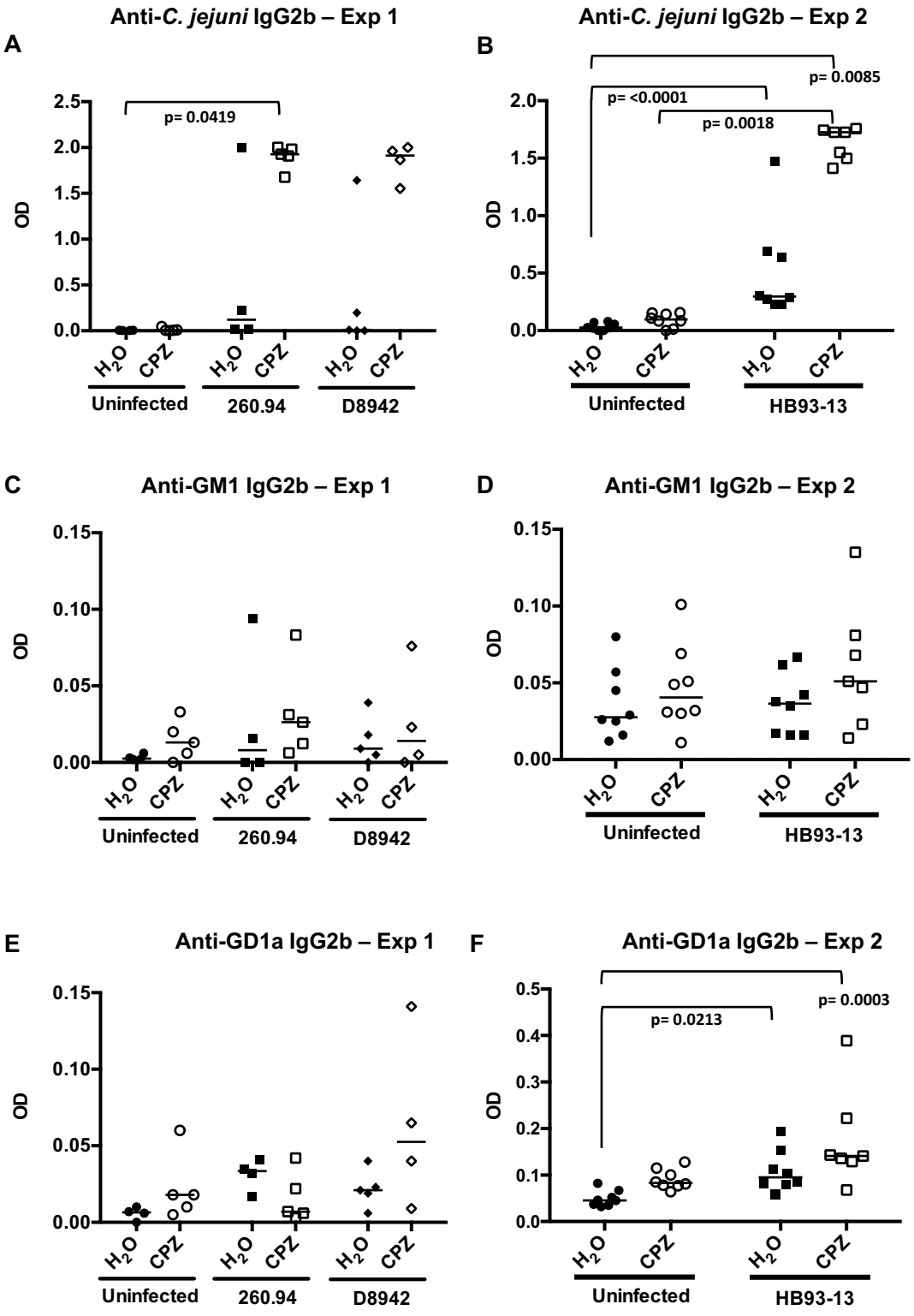

Fig. 8. Type 17 antibody responses were enhanced by antibiotic treatment in a strain specific manner. Plasma antibodies reactive with gangliosides (GM1 and GD1a) and *C. jejuni* antigen were measured via indirect ELISA. Biotinylated goat anti-mouse secondary antibodies were used to determine IgG subclass. Each symbol represents a single animal; bars represent group means. Data represent 4–5 mice per group (pilot and experiment 1) or 6–8 mice (experiment 2); and the means of 3 replicate wells per sample were analyzed by Kruskal-Wallis test on ranks with Dunn's post test and $p < 0.05$ was considered statistically significant.

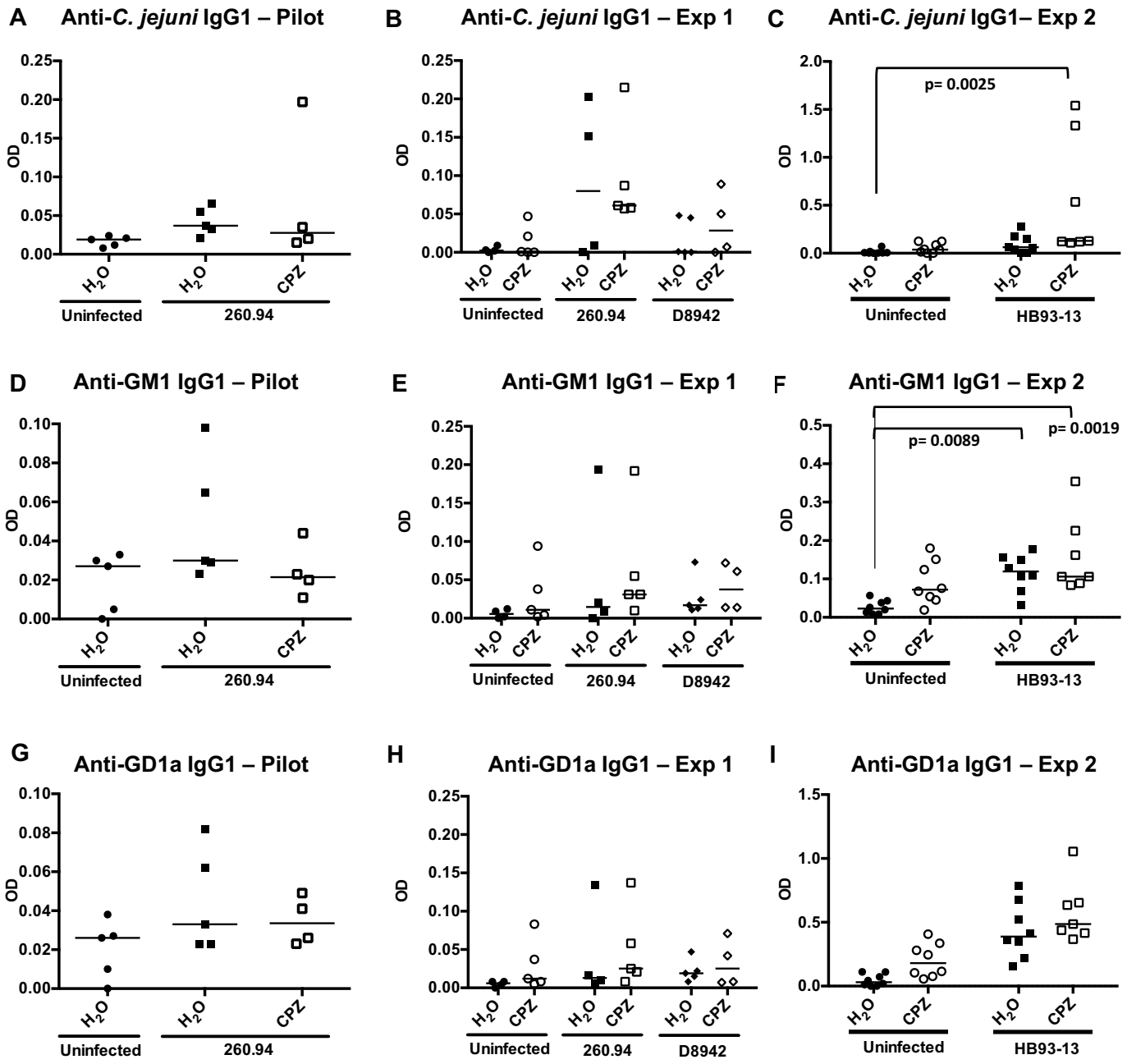

Fig. 9. *C. jejuni* HB93–13 but not 260.94 or D8942 elicited Type 2 anti-*C. jejuni* and anti-ganglioside antibody responses. Plasma antibodies reactive with *C. jejuni* antigen and gangliosides (GM1 and GD1a) were measured via indirect ELISA. Biotinylated goat anti-mouse secondary antibodies were used to determine the IgG subclass. Each symbol represents a single animal; bars represent group medians. Data represent 4–5 mice per group (pilot and experiment 1) or 6–8 mice (experiment 2); and the means of 3 replicate wells per sample were analyzed by Kruskal-Wallis test on ranks with Dunn's post test and $p < 0.05$ was considered statistically significant. Panels A, D, and C show results from the pilot experiment, panels B, E and H show results from experiment 1 and panels C, F and I show results from experiment 2. Significant elevations of anti-*C. jejuni* IgG1 antibody was seen only in *C. jejuni* HB-93.13 infected mice treated with CPZ (panel C), while anti-GM1 IgG1 antibodies were seen in *C. jejuni* HB-93.13 infected mice given either sterile water or CPZ treated water (panel F).

enteritis used in previous work does have GM1 and GM2 mimics but did not appear to increase anti-ganglioside antibodies in infected mice (Malik et al., 2014). The presence of antibodies cross-reactive with *C. jejuni* and peripheral nerve gangliosides confirms *C. jejuni*-mediated-autoimmunity which is exacerbated by antibiotic treatment in our mouse model. If in fact these antibodies initiate the immune attack on nerve tissue that is hypothesized to cause GBS, our results suggest that depleted microbiota may not only modulate *C. jejuni*-meditated-autoimmunity but may also enhance host susceptibility to GBS.

Previously we determined that contrasting immune responses mediate *Campylobacter jejuni* induced colitis and autoimmunity in C57BL/6 IL-10 deficient mice, dependent upon the infecting strain (Malik et al., 2014). *C. jejuni* GBS patient strains induced no to mild colitis associated with blunted Type 1/17 but enhanced Type 2

Table 2
Comparative analysis of anti-ganglioside antibody and F4/80 positive macrophages staining in Experiments 1 and 2.

A

EXPERIMENT 1	ANTI-GANGLIOSIDE ANTIBODIES						MACROPHAGES	
	IgG1		IgG2b		IgG2c			
TREATMENT	GM1	GD1a	GM1	GD1a	GM1	GD1a	DRG	SN
TSB								
TSB								
TSB								
TSB								
CPZ								
CPZ								
CPZ								
CPZ								
CPZ								
Cj 260.94								
Cj 260.94								
Cj 260.94								
Cj 260.94								
Cj 260.94+CPZ								
Cj 260.94+CPZ								
Cj 260.94+CPZ								
Cj 260.94+CPZ								
Cj 260.94+CPZ								
Cj D8942								
Cj D8942								
Cj D8942								
Cj D8942								
Cj D8942								
Cj D8942+CPZ								
Cj D8942+CPZ								
Cj D8942+CPZ								
Cj D8942+CPZ								

B

EXPERIMENT 2	ANTI-GANGLIOSIDE ANTIBODIES						MACROPHAGES	
	IgG1		IgG2b		IgG2c			
TREATMENT	GM1	GD1a	GM1	GD1a	GM1	GD1a	DRG	SN
TSB								
TSB								
TSB								
TSB								
TSB								
TSB								
TSB								
TSB								
CPZ								
CPZ								
CPZ								
CPZ								
CPZ								
CPZ								
CPZ								
CPZ								
Cj HB93.13								
Cj HB93.13								
Cj HB93.13								
Cj HB93.13								
Cj HB93.13								
Cj HB93.13								
Cj HB93.13								
Cj HB93.13								
Cj HB93.13+CPZ								
Cj HB93.13+CPZ								
Cj HB93.13+CPZ								
Cj HB93.13+CPZ								
Cj HB93.13+CPZ								
Cj HB93.13+CPZ								
Cj HB93.13+CPZ								

A) Results from Experiment 1 at 5 weeks post infection and B) results from Experiment 2 at 7 weeks post infection. Represents individual positive antibody and F4/80 responses. A score two or more standard deviations from the mean of the uninfected + H_2O was deemed a positive response. Yellow color indicates significantly elevated antiganglioside antibodies of that specificity and isotype. Orange indicates the presence of significant numbers of macrophages in dorsal root ganglia or sciatic nerves of mice.

responses; Type 2 but not Type 1/17 antibodies cross-reacted with peripheral nerve gangliosides, demonstrating autoimmunity. In this study we tested whether colonization resistance afforded by commensal gut microbiota plays an important role in susceptibility to GBS. We found that *C. jejuni* strains from GBS patients resistant to the broad-spectrum antibiotic CPZ produced severe Type 1/17 colitis when C57BL/6 IL-$10^{-/-}$ mice were treated with CPZ, which decreased complexity and abundance of the gut microbiota. In mice infected with *C. jejuni* 260.94 given CPZ, colitis was mediated by T_H1 cells that peaked at 5 weeks post infection. However, it was not surprising that these cellular responses did not rise to significance at 7 weeks post infection because by this time most of the severely affected animals had already reached humane endpoints that necessitated euthanasia. Other GBS-associated *C. jejuni* strains, HB93-13 and D8942, produced similar but less pronounced cellular responses in the proximal colon in infected CPZ treated mice; results were statistically significant in some experiments but not others. Thus, we can accept our hypothesis that depletion of gut microbiota with a broad-spectrum antibiotic increases colonization and gastroenteritis by GBS patient strains of *C. jejuni*.

In these studies, Cefoperazone treatment increased colonization of *C. jejuni* strains. However, anti-*C. jejuni* IgG1, IgG2c responses, and Th1 and Th2 cell frequencies in this treatment groups were not always consistent with bacterial colonization. Some of the variation in these responses could be time dependent differences of when the mice generated peak responses since we only measured at necropsy. Some of the variation could also be dependent upon the infecting *C. jejuni* strain. Furthermore, it is possible that other bacteria are facilitated by Cefoperazone treatment. Cefoperazone treatment significantly decreased the majority of bacterial groups in the GI tract in our experiment so that they were not detectable by qPCR for major bacterial groups. However, in another study *Escherichia coli* and *Lactobacillus* were still present at very low levels and were detectable two weeks after Cefoperazone treatment was stopped (Schubert et al., 2015). It is also possible that other GI bacteria possess ganglioside mimics that could intensify the GBS outcomes. Further study is needed to pursue these questions.

Consistent with previous results from other labs, our work demonstrates that *C. jejuni* strains from GBS patients can produce gastroenteritis under depleted microbiota conditions and that antibiotic depletion of the gut microbiota alters immune responses to these GBS strains of *C. jejuni* in a way that exacerbates colitis. Based on the anti-*C. jejuni* and anti-ganglioside specific antibody isotypes observed in these studies this outcome most likely occurred by a similar IFNγ-dependent mechanism, and formation of anti-ganglioside antibodies. In addition, we observed that the microbiota is not the only factor mediating the host immune response to *C. jejuni* infection; our results show that anti-ganglioside antibody responses varied by the infecting *C. jejuni* strain.

Notably, antibiotic depletion of gut microbiota exacerbated anti-ganglioside responses resulting in significant Ig2b and IgG2c anti-ganglioside antibodies in C57BL/6 IL-10 deficient mice, consistent with enhanced inflammation associated with antibiotic treatment. The IgG1 antibodies that we observed in these mice are of particular interest because previous reports on GBS patients have identified GM1 IgG1 antibodies as predictors of severe outcomes and prolonged recovery in humans (Koga et al., 2003). Because HB93–13 elicited significant IgG1 anti-ganglioside antibody responses in the same genotype of mice in previous work (Malik et al., 2014), we expected that these responses would be repeated here and would be exacerbated by antibiotic treatment, which is what was observed. More work is needed to understand the exact mechanism of nerve damage in this model.

Severe colitis may cause hunched posture of the mice, which may be taken for a sign of neurological disease by an untrained individual scoring the mice for clinical signs. To prevent this mistake, we use a scoring criteria (St Charles et al., 2017) and veterinarians score clinical signs in the mice. We also have a separate pathologist score the gastrointestinal lesions. Both methods are done in a blinded fashion so that the veterinarians do not have the identity of the treatment group as they conduct their assessments. For neurologic assessments, a trained individual videotapes the mice in an open field test and then a veterinarian scores the blinded videotape. We apply a scoring criteria using JWatcher software to sum each neurologic feature so that they can be compared between groups. Some of the mice with neurologic signs did have high colitis scores. However, the majority of mice with neurologic signs did not have colitis scores of note. Generally, C57BL/6 IL-10 deficient mice develop mild GBS signs where nerve macrophage numbers peaking around 7 weeks post infection (Malik et al., 2014). Yet we had to euthanize the mice at a time when both colitis and GBS were present and so we chose 5 weeks PI. It is clear from the many neurologic manifestations, that a significant number of *C. jejuni* infected mice given antibiotics had some neurological signs.

6. Conclusions

In this study, we have identified antibiotic depleted gut microbiota as a factor in *C. jejuni* mediated-autoimmunity. We show that antibiotic treatment enhanced *Campylobacter* T cell mediated inflammation, manifesting as exacerbated enteric lesions. While significant levels of anti-*C. jejuni* antibodies and anti-GM1 and GD1a ganglioside antibodies were produced in infected CPZ treated mice, the antiganglioside antibodies were mainly of Type 1/17 isotypes and did not correlate with significant levels of macrophages in the peripheral nerves indicative of GBS. Together, these data indicate that factors such as gut microbiota can influence T helper cell differentiation and autoimmune outcomes to an enteric pathogen. Furthermore, antibiotic depletion drove severe *Campylobacter jejuni*-mediated Type 1/17 colitis by two previously non-inflammatory GBS patient strains that heretofore had produced little or no colitis in this model.

Antibiotic treatment depleted the gut microbiota and increased the number of resistant *C. jejuni* in the colon lumen and gut wall. In infected mice antibiotic treatment enhanced the frequency and severity of colitis and exacerbated anti-ganglioside autoantibody responses and neurologic signs. Antibiotic depletion of gut microbiota was a critical factor in the manifestation of very severe enteric disease in this model and increased the number of mice with antiganglioside antibodies, but it was more difficult to evaluate GBS-associated nerve damage because humane endpoints were reached before nerve lesions could fully form. Despite significant increases in Type 2 indicators in infected mice given CPZ, microbiota depletion had greater effects on enhancing colitis than on enhancing nerve lesions. Nevertheless, when all three GBS indicators evaluated were considered together (neurological phenotype, anti-ganglioside antibodies, and numbers of macrophage in dorsal root ganglia and sciatic nerve), mice infected with *C. jejuni* HB93-13 and treated with cefoperazone did exhibit a trend toward greater severity of GBS-like disease manifestations compared to non-antibiotic treated mice.

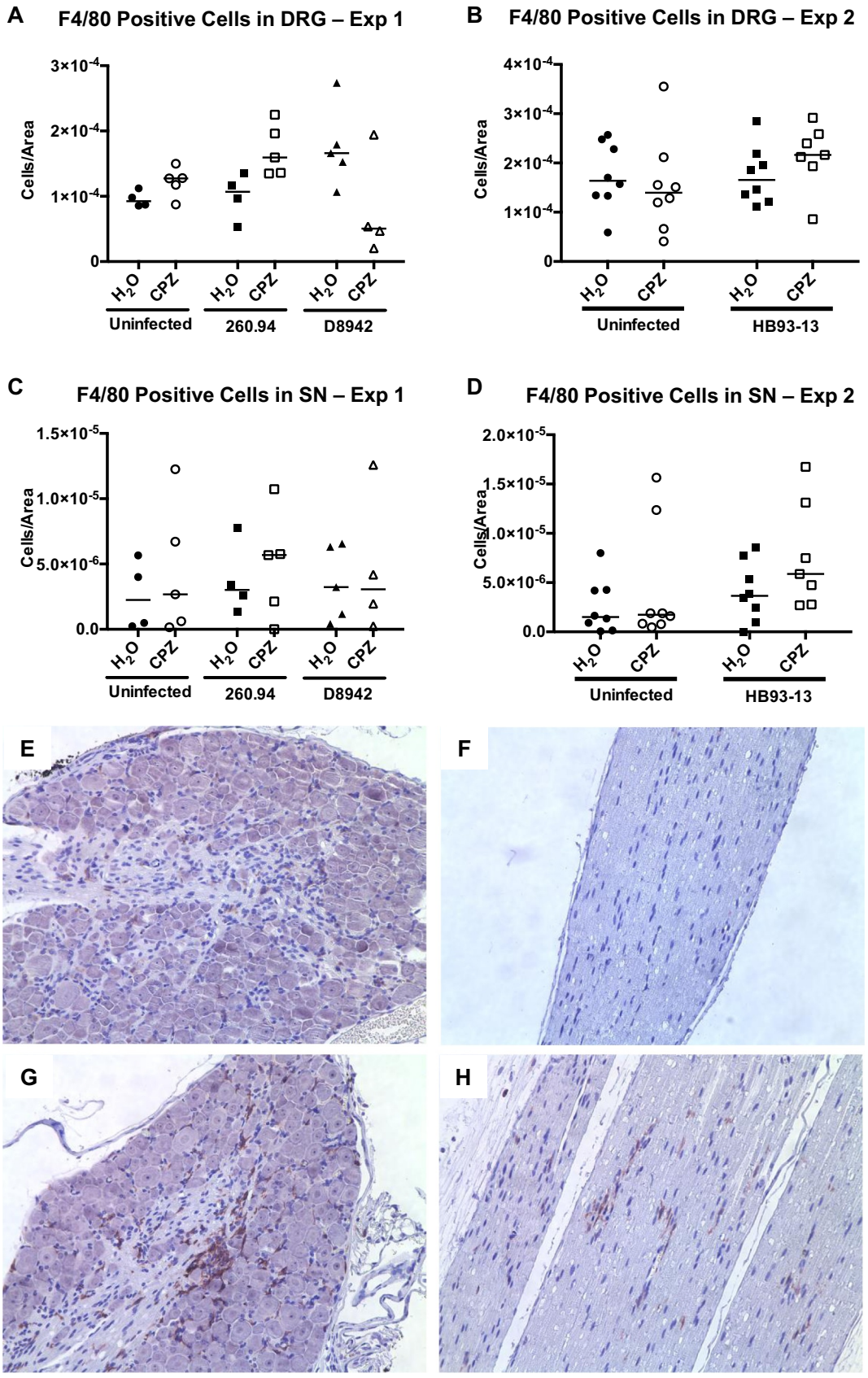

Fig. 10. Anti-F480 immunohistochemical labeling of sciatic nerves and dorsal root ganglia. Panels A and B show counts of F4/80 positive cells in the dorsal root ganglia of mice from Experiment 1 and 2, respectively. Panels C and D show counts of F4/80 cells in the sciatic nerves of mice in Experiment 1 and 2, respectively. Data represent 4–8 animals per group with the median values. No significant differences were detected. NS = Not significant. Panels *E*-H show examples of stained peripheral nerve sections. Panel E shows a dorsal root ganglia section from an uninfected mouse. Panel F shows a sciatic nerve section from an uninfected mouse. Panels G (dorsal root ganglion section) and F (sciatic nerve section) are from a *C. jejuni* 260.94 infected mouse both showing numerous F4/80 positive macrophages.

Mouse Number	Sex	Inoculum	CPZ Tx	Colitis Score	Maximum neurological phenotype score	Anti-*C. jejuni* IgG1	Anti-GM1 IgG1	Anti-GD1a IgG1	F4/80 Sciatic Score	F4/80 DRG Score
9234	F	TSB		0	0	0.29	0.07	0.15	1	68
9258	F	TSB		0	1	0.29	0.31	0.17	13	24
9273	F	TSB		0	0	0.36	0.31	0.15	5	39
9269	F	TSB		0	1	0.30	0.19	0.12	26	91
9228	M	TSB		0	1	0.28	0.21	0.12	28	217
9254	M	TSB		0	1	0.29	0.19	0.12	89	167
9261	M	TSB		0	0	0.29	0.24	0.13	7	17
9267	M	TSB		0	2	0.29	0.21	0.01	42	77
Group average						0.30	0.22	0.12	26	88
9270	F	TSB	CPZ	0	1	0.32	0.31	0.18	17	128
9235	F	TSB	CPZ	0	1	0.41	0.53	0.30	104	126
9259	F	TSB	CPZ	0	1	0.41	0.60	0.29	10	7
9274	F	TSB	CPZ	0	1	0.37	0.48	0.23	1	20
9229	M	TSB	CPZ	0	2	0.28	0.30	0.16	137	39
9255	M	TSB	CPZ	0	2	0.28	0.27	0.12	10	84
9262	M	TSB	CPZ	0	2	0.30	0.25	0.15	9	39
9268	M	TSB	CPZ	0	1	0.32	0.24	0.18	4	87
Group average						0.34	0.37	0.20	37	66
9271	F	HB93-13		0	1	0.34	0.56	0.29	19	120
9232	F	HB93-13		0	3	0.28	0.36	0.14	41	33
9256	F	HB93-13		0	1	0.56	0.98	0.25	6	131
9275	F	HB93-13		0	5	0.35	0.61	0.21	0	59
9264	F	HB93-13		1	4	0.46	0.72	0.21	97	175
9230	M	HB93-13		0	2	0.29	0.55	0.24	58	133
9276	M	HB93-13		0	3	0.43	0.88	0.26	13	129
9263	M	HB93-13		0	5	0.33	0.42	0.17	56	129
Group average						0.38	0.64	0.22	36	114
9257	F	HB93-13	CPZ	1	6	0.41	0.85	0.27	23	27
9265	F	HB93-13	CPZ	1	1	0.40	0.57	0.22	28	235
9272	F	HB93-13	CPZ	2	2	0.42	0.69	0.21	37	153
9233	F	HB93-13	CPZ	2	4	1.80	1.25	0.50	95	302
9231	M	HB93-13	CPZ	2	3	1.60	0.62	0.20	19	284
9277	M	HB93-13	CPZ	2	4	0.82	0.84	0.33	100	68
9260	M	HB93-13	CPZ	2	4	0.41	0.64	0.19	53	223
Group average						0.84	0.78	0.27	51	185
(average + 2 X standard deviation), TSB only group						0.35	0.37	0.22	84	229

Fig. 11. Summary of disease indicators and immunological data for each animal in Experiment 2. Colitis scores are given as ranks 0 = normal, 1 = mild colitis (pale orange), and 2 = severe colitis (dark orange). The number of abnormal neurological findings is given for each mouse at each phenotyping day and scores range from 1 in pale blue through darker shades of blue to the darkest at 6 abnormal findings. Anti-*Campylobacter* and antiganglioside antibodies (GM1 IgG1, GD1 IgG1) are given as average optical density values. The yellow colored cells for these antibody responses indicate values greater than the sum of the mean of the TSB only group plus twice the standard deviation of that group (values given in the last row). (For interpretation of the references to color in this figure legend, the reader is referred to the web version of this article.)

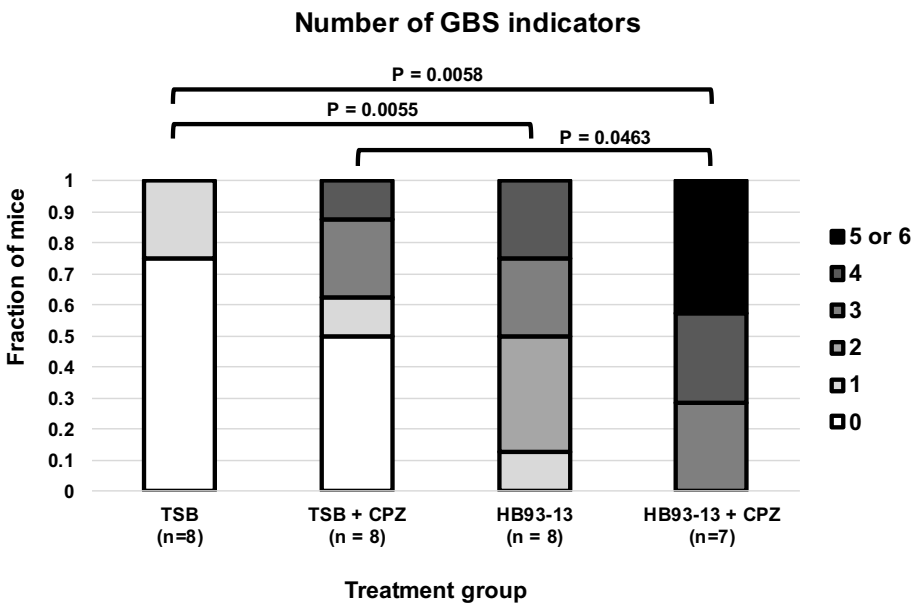

Fig. 12. Overall assessment of Guillain Barré syndrome indicators including phenotype, all anti-GM1 IgG1 antibody responses and macrophages in the dorsal root ganglion and the sciatic nerve. Fig. 12 shows the distribution of these scores in the four treatment groups. Kruskal Wallis one-way ANOVA on ranks was significant for these data ($P = 0.0004$). Mann-Whitney pairwise comparisons that were significant after Bonferroni correction for multiple comparisons were non-antibiotic-treated TSB-inoculated mice versus non-antibiotic-treated HB93-13-inoculated mice ($P = 0.0055$), non-antibiotic-treated TSB-inoculated mice versus antibiotic-treated HB93-13-inoculated mice ($P = 0.0058$), and non-antibiotic-treated TSB-inoculated mice vs antibiotic-treated HB93-13- inoculated mice ($P = 0.0463$). No other pairwise comparisons were significant; the P value for the comparison of non-antibiotic-treated HB93-13-inoculated mice versus antibiotic-treated HB93-13-inoculated mice was 0.1257.

Declaration of Competing Interest

None.

Acknowledgments

The authors thank Collette Fitzgerald (CDC) for providing *C. jejuni* strain D8942. Thanks go to the Michigan State University Investigative Histopathology Laboratory for slide preparation and immunohistochemistry. In addition, we would like to thank Jean Brudvig, Leslie Dybas, and Alexander Ethridge for technical support. These studies were funded in whole with federal funds from NIAID, NIH, Department of Health and Human Services, under grant number U19AI090872 Enterics Research Investigational Network, Cooperative Research Center. Research salary and travel awards for Phillip T. Brooks were supported by the Institute for Integrative Toxicology at Michigan State University and a National Institutes of Environmental Health Sciences of the NIH, Department of Health and Human Services grant number T32ES007255 to Michigan State University.

References

Antonopoulos, D.A., Huse, S.M., Morrison, H.G., Schmidt, T.M., Sogin, M.L., Young, V.B., 2009. Reproducible community dynamics of the gastrointestinal microbiota following antibiotic perturbation. Infect. Immun. 77, 2367–2375.

Bai, Y., Liu, R., Huang, D., La Cava, A., Tang, Y.Y., Iwakura, Y., Campagnolo, D.I., Vollmer, T.L., Ransohoff, R.M., Shi, F.D., 2008. CCL2 recruitment of IL-6-producing CD11b+ monocytes to the draining lymph nodes during the initiation of Th17-dependent B cell-mediated autoimmunity. Eur. J. Immunol. 38, 1877–1888.

Bristol, I.J., Farmer, M.A., Cong, Y., Zheng, X.X., Strom, T.B., Elson, C.O., Sundberg, J.P., Leiter, E.H., 2000. Heritable susceptibility for colitis in mice induced by IL-10 deficiency. Inflamm. Bowel Dis. 6, 290–302.

Caroline, A.S., Wayne, S.R., Kevin, W.E., 2012. NIH image to ImageJ: 25 years of image analysis. Nat. Methods 9, 671–675.

CDC, 2014. Campylobacter: General Information.

Centers for Disease Control and Prevention, 2013. Antibiotic resistant threats in the United States, 2013.

Chang, C., Miller, J.F., 2006. Campylobacter jejuni colonization of mice with limited enteric flora. Infect. Immun. 74, 5261–5271.

Dutka-Malen, S., Evers, S., Courvalin, P., 1995. Detection of glycopeptide resistance genotypes and identification to the species level of clinically relevant enterococci by PCR. J. Clin. Microbiol. 33, 24–27.

Garg, A.X., Pope, J.E., Thiessen-Philbrook, H., Clark, W.F., Ouimet, J., Investigators, W.H.S., 2008. Arthritis risk after acute bacterial gastroenteritis. Rheumatology (Oxford) 47, 200–204.

Germann, T., Bongartz, M., Dlugonska, H., Hess, H., Schmitt, E., Kolbe, L., Kölsch, E., Podlaski, F.J., Gately, M.K., Rüde, E., 1995. Interleukin-12 profoundly up-regulates the synthesis of antigen-specific complement-fixing IgG2a, IgG2b and IgG3 antibody subclasses in vivo. Interleukin-12 profoundly up-regulates the synthesis of antigen-specific complement-fixing IgG2a, IgG2b and IgG3 antibody subclasses in vivo 25.

Gilbert, M., Karwaski, M.F., Bernatchez, S., Young, N.M., Taboada, E., Michniewicz, J., Cunningham, A.M., Wakarchuk, W.W., 2002. The genetic bases for the variation in the lipo-oligosaccharide of the mucosal pathogen, *Campylobacter jejuni*. Biosynthesis of sialylated ganglioside mimics in the core oligosaccharide. J. Biol. Chem. 277, 327–337.

Gruenewald, R., Ropper, A.H., Lior, H., Chan, J., Lee, R., Molinaro, V.S., 1991. Serologic evidence of *Campylobacter jejuni*/coli enteritis in patients with Guillain-Barre syndrome. Arch. Neurol. 48, 1080–1082.

Guo, B., Lin, J., Reynolds, D.L., Zhang, Q., 2010. Contribution of the multidrug efflux transporter CmeABC to antibiotic resistance in different *Campylobacter* species. Foodborne Pathog. Dis. 7, 77–83.

Hatzipetros, T., Kidd, J.D., Moreno, A.J., Thompson, K., Gill, A., Vieira, F.G., 2015. A quick phenotypic neurological scoring system for evaluating disease progression in the SOD1-G93A mouse model of ALS. J. Visual. Exp. 104, 1–6.

Houliston, R., Vinogradov, E., Dzieciatkowska, M., Li, J., Michael, F., Karwaski, M.-F., Brochu, D., Jarrell, H., Parker, C., Yuki, N., Mandrell, R., Gilbert, M., 2011. Lipooligosaccharide of *Campylobacter jejuni*: similarity with multiple types of mammalian glycans beyond gangliosides. J. Biol. Chem. 286.

Hughes, R.A., Rees, J.H., 1997. Clinical and epidemiologic features of Guillain-Barré syndrome. J. Infect. Dis. 176 (Suppl. 2), S92–S98.

Jackson, B.R., Zegarra, J.A., López-Gatell, H., Sejvar, J., Arzate, F., Waterman, S., Núñez, A.S., López, B., Weiss, J., Cruz, R.Q., Murrieta, D.Y.L., Luna-Gierke, R., Heiman, K., Vieira, A.R., Fitzgerald, C., Kwan, P., Zárate-Bermúdez, M., Talkington, D., Hill, V.R., Mahon, B., Team, G.B.S.O.I., 2013. Binational outbreak of Guillain-Barré syndrome associated with *Campylobacter jejuni* infection, Mexico and USA, 2011. Epidemiol. Infect. 142, 1089–1099.

Kamada, N., Chen, G.Y., Inohara, N., Nunez, G., 2013. Control of pathogens and pathobionts by the gut microbiota. Nat. Immunol. 14, 685–690.

Kim, O.G., Hans, L.N., Henrik, C.S., Tove, E., Brian, K., Henrik, N., 2009. Increased short- and long-term risk of inflammatory bowel disease after *Salmonella* or *Campylobacter* gastroenteritis. Gastroenterology 137, 495–501.

Koga, M., Yuki, N., Hirata, K., Morimatsu, M., Mori, M., Kuwabara, S., 2003. Anti-GM1 antibody IgG subclass: a clinical recovery predictor in Guillain-Barré syndrome. Neurology 60, 1514–1518.

Leary, S., Underwood, W., Anthony, R., Carter, S., Corey, D., Grandin, T., Greenacre, C.B., Gwaltney-Bran, S., McCrackin, M.A., Meyer, R., Miller, D., Shearer, J., Yang, R., 2013. AVMA Guidelines for the Euthanasia of Animals: 2013 Edition. American Veterinary Medical Association, pp. 1–102.

Lin, J., Michel, L.O., Zhang, Q., 2002. CmeABC functions as a multidrug efflux system in *Campylobacter jejuni*. Antimicrob. Agents Chemother. 46, 2124–2131.

Linton, D., Owen, R., Stanley, J., 1996. Rapid identification by PCR of the genus *Campylobacter* and of five Campylobacter species enteropathogenic for man and animals. Res. Microbiol. 147, 707–718.

Louwen, R., Horst-Kreft, D., de Boer, A.G., van der Graaf, L., de Knegt, G., Hamersma, M., Heikema, A.P., Timms, A.R., Jacobs, B.C., Wagenaar, J.A., Endtz, H.P., van der Oost, J., Wells, J.M., Nieuwenhuis, E.E., van Vliet, A.H., Willemsen, P.T., van Baarlen, P., van Belkum, A., 2013. A novel link between *Campylobacter jejuni* bacteriophage defence, virulence and Guillain-Barre syndrome. Eur. J. Clin. Microbiol. Infect. Dis. 32, 207–226.

Ludbrook, J., 1998. Multiple comparison procedures updated. Clin. Exp. Pharmacol. Physiol. 25, 1032–1037.

Malik, A., Sharma, D., St Charles, J., Dybas, L.A., Mansfield, L.S., 2014. Contrasting immune responses mediate *Campylobacter jejuni*-induced colitis and autoimmunity.

Mucosal Immunol. 7, 802–817.
Mansfield, L.S., Bell, J.A., Wilson, D.L., Murphy, A.J., Elsheikha, H.M., Rathinam, V.A., Fierro, B.R., Linz, J.E., Young, V.B., 2007. C57BL/6 and congenic interleukin-10-deficient mice can serve as models of *Campylobacter jejuni* colonization and enteritis. Infect. Immun. 75, 1099–1115.
McKeel, R., Douris, N., Foley, P., Feldman, S., 2002. Comparison of an espB gene fecal polymerase chain reaction assay with bacteriologic isolation for detection of Citrobacter rodentium infection in mice. Comp. Med. 52, 439–444.
Melis, J.P., Strumane, K., Ruuls, S.R., Beurskens, F.J., Schuurman, J., Parren, P.W., 2015. Complement in therapy and disease: regulating the complement system with antibody-based therapeutics. Mol. Immunol. 67, 117–130.
Moore, J.E., Barton, M.D., Blair, I.S., Corcoran, D., Dooley, J.S., Fanning, S., Kempf, I., Lastovica, A.J., Lowery, C.J., Matsuda, M., McDowell, D.A., McMahon, A., Millar, B.C., Rao, J.R., Rooney, P.J., Seal, B.S., Snelling, W.J., Tolba, O., 2006. The epidemiology of antibiotic resistance in *Campylobacter*. Microb. Infect. 8, 1955–1966.
Nagalingam, N.A., Robinson, C.J., Bergin, I.L., Eaton, K.A., Huffnagle, G.B., Young, V.B., 2013. The effects of intestinal microbial community structure on disease manifestation in IL-10−/− mice infected with Helicobacter hepaticus. Microbiome 1, 15.
O'Loughlin, J.L., Samuelson, D.R., Braundmeier-Fleming, A.G., White, B.A., Haldorson, G.J., Stone, J.B., Lessmann, J.J., Eucker, T.P., Konkel, M.E., 2015a. The intestinal microbiota influences *Campylobacter jejuni* colonization and Extraintestinal dissemination in mice. Appl. Environ. Microbiol. 81 (14), 4642–4650.
O'Loughlin, J.L., Samuelson, D.R., Braundmeier-Fleming, A.G., White, B.A., Haldorson, G.J., Stone, J.B., Lessmann, J.J., Eucker, T.P., Konkel, M.E., 2015b. The intestinal microbiota influences *Campylobacter jejuni* colonization and extraintestinal dissemination in mice. Appl. Environ. Microbiol. 81, 4642–4650.
Parker, C.T., Horn, S.T., Gilbert, M., Miller, W.G., Woodward, D.L., Mandrell, R.E., 2005. Comparison of *Campylobacter jejuni* Lipooligosaccharide biosynthesis loci from a variety of sources. J. Clin. Microbiol. 43, 27712781.
Prendergast, M., Lastovica, A., Moran, A., 1998. Lipopolysaccharides from Campylobacter jejuni O:41 strains associated with Guillain-Barré syndrome exhibit mimicry of GM1 ganglioside. Infect. Immunity 66.
Rathinam, V.A., Hoag, K.A., Mansfield, L.S., 2008. Dendritic cells from C57BL/6 mice undergo activation and induce Th1-effector cell responses against *Campylobacter jejuni*. Microb. Infect. 10 (12-13), 1316–1324.
Rathinam, V.A., Appledorn, D.M., Hoag, K.A., Amalfitano, A., Mansfield, L.S., 2009. Campylobacter jejuni-induced activation of dendritic cells involves cooperative signaling through TLR4-MyD88 and TLR4-TRIF axes. Infect. Immun. 77 (6), 2499–2507.
Riley, L., Franklin, C., Hook Jr., R., Besch-Williford, C., 1996. Identification of murine helicobacters by PCR and restriction enzyme analyses. J. Clin. Microbiol. 34, 942.
Scallan, E., Griffin, P.M., Angulo, F.J., Tauxe, R.V., Hoekstra, R.M., 2011. Foodborne illness acquired in the United States–unspecified agents. Emerg. Infect. Dis. 17, 16–22.
Schonberg-Norio, D., Mattila, L., Lauhio, A., Katila, M.L., Kaukoranta, S.S., Koskela, M., Pajarre, S., Uksila, J., Eerola, E., Sarna, S., Rautelin, H., 2010. Patient-reported complications associated with *Campylobacter jejuni* infection. Epidemiol. Infect. 138, 1004–1011.
Schubert, A.M., Sinani, H., Schloss, P.D., 2015. Antibiotic-induced alterations of the murine gut microbiota and subsequent effects on colonization resistance against *Clostridium difficile*. MBio 6, e00974.
Sekirov, I., Tam, N.M., Jogova, M., Robertson, M.L., Li, Y., Lupp, C., Finlay, B.B., 2008. Antibiotic-induced perturbations of the intestinal microbiota alter host susceptibility to enteric infection. Infect. Immun. 76, 4726–4736.
Sheikh, K.A., Ho, T.W., Nachamkin, I., Li, C.Y., Cornblath, D.R., Asbury, A.K., Griffin, J.W., McKhann, G.M., 1998a. Molecular mimicry in Guillain-Barré syndrome. Ann. N. Y. Acad. Sci. 845, 307–321.
Sheikh, K.A., Nachamkin, I., Ho, T.W., Willison, H.J., Veitch, J., Ung, H., Nicholson, M., Li, C.Y., Wu, H.S., Shen, B.Q., Cornblath, D.R., Asbury, A.K., McKhann, G.M., Griffin, J.W., 1998b. *Campylobacter jejuni* lipopolysaccharides in Guillain-Barré syndrome: molecular mimicry and host susceptibility. Neurology 51, 371–378.
St Charles, J.L., Bell, J.A., Gadsden, B.J., Malik, A., Cooke, H., Van de Grift, L.K., Kim, H.Y., Smith, E.J., Mansfield, L.S., 2017. Guillain Barre syndrome is induced in non-obese diabetic (NOD) mice following *Campylobacter jejuni* infection and is exacerbated by antibiotics. J. Autoimmun. 77, 11–38.
Stahl, M., Ries, J., Vermeulen, J., Yang, H., Sham, H.P., Crowley, S.M., Badayeva, Y., Turvey, S.E., Gaynor, E.C., Li, X., Vallance, B.A., 2014. A novel mouse model of *Campylobacter jejuni* gastroenteritis reveals key pro-inflammatory and tissue protective roles for Toll-like receptor signaling during infection. PLoS Pathog. 10, e1004264.
Theriot, C., Koenigsknecht Jr., M., Hatton, G., Nelson, A., Li, B., Huffnagle, G., Li, J., Young, V., 2014. Antibiotic-induced shifts in the mouse gut microbiome and metabolome increase susceptibility to *Clostridium difficile* infection. Nat. Commun. 5.
Uncini, A., Shahrizaila, N., Kuwabara, S., 2017. Zika virus infection and Guillain-Barre syndrome: a review focused on clinical and electrophysiological subtypes. J. Neurol. Neurosurg. Psychiatry 88, 266–271.
van den Berg, B., Walgaard, C., Drenthen, J., Fokke, C., Jacobs, B.C., van Doorn, P.A., 2014. Guillain-Barre syndrome: pathogenesis, diagnosis, treatment and prognosis. Nat. Rev. Neurol. 10, 469–482.
Willison, H.J., Jacobs, B.C., van Doorn, P.A., 2016. Guillain-Barre syndrome. Lancet 388, 717–727.
Wilson, D.L., Abner, S.R., Newman, T.C., Mansfield, L.S., Linz, J.E., 2000. Identification of ciprofloxacin-resistant *Campylobacter jejuni* by use of a fluorogenic PCR assay. J. Clin. Microbiol. 38, 3971–3978.
Yin, J., Wang, S., Liao, S.-X.X., Peng, X., He, Y., Chen, Y.-R.R., Shen, H.-F.F., Su, J., Chen, Y., Jiang, Y.-X.X., Zhang, G.-X.X., Zhou, H.-W.W., 2015. Different dynamic patterns of β-lactams, quinolones, glycopeptides and macrolides on mouse gut microbial diversity. PloS O 10.
Young, K.T., Davis, L.M., Dirita, V.J., 2007. *Campylobacter jejuni*: molecular biology and pathogenesis. Nat. Rev. Microbiol. 5, 665–679.
Yuki, N., 2012. Guillain-Barré syndrome and anti-ganglioside antibodies: a clinician-scientist's journey. Proc. Jpn. Acad. Series B Phys. Biol. Sci. 88.
Yuki, N., Hartung, H.P., 2012. Guillain-Barre syndrome. N. Engl. J. Med. 366, 2294–2304.
Yuki, N., Taki, T., Inagaki, F., Kasama, T., Takahashi, M., Saito, K., Handa, S., Miyatake, T., 1993. A bacterium lipopolysaccharide that elicits Guillain-Barré syndrome has a GM1 ganglioside-like structure. J. Exp. Med. 178.
Zhang, J., Li, J., Hu, W., 2013. Myasthenia gravis and Guillain-Barré co-occurrence syndrome. In: Myasthenia gravis and Guillain-Barré co-occurrence syndrome.
Zia, S., Wareing, D., Sutton, C., Bolton, E., Mitchell, D., Goodacre, J.A., 2003. Health problems following *Campylobacter jejuni* enteritis in a Lancashire population. Rheumatology (Oxford) 42, 1083–1088.